Journal of Hazardous Materials 480 (2024) 136128

Contents lists available at ScienceDirect

Journal of Hazardous Materials

journal homepage: www.elsevier.com/locate/jhazmat

Bacterial bioaugmentation for paracetamol removal from water and sewage sludge. Genomic approaches to elucidate biodegradation pathway

A. Lara-Moreno [a,b], A. Vargas-Ordóñez [a], J. Villaverde [a], F. Madrid [a], J.D. Carlier [c], J.L. Santos [d], E. Alonso [d], E. Morillo [a,*]

[a] Institute of Natural Resources and Agrobiology of Seville, Department of Agrochemistry, Environmental Microbiology and Soil Conservation, Spanish National Research Council (IRNAS-CSIC), Seville, Spain
[b] Department of Microbiology and Parasitology, Faculty of Pharmacy, University of Seville, Seville, Spain
[c] Centre of Marine Sciences (CCMAR), University of Algarve, Gambelas Campus, Building 7, Faro 8005-139, Portugal
[d] Departamento de Química Analítica, Escuela Politécnica Superior, Universidad de Sevilla, C/ Virgen de África, 7, 41011 Seville, Spain

HIGHLIGHTS

- Wide ranges of APAP concentrations degraded by *P. extremaustralis* CSW01 / *S. stutzeri* CSW02 at various temperatures and pHs.
- CSW01 mineralized APAP (500 ppm) up to 74 % in consortia with *M. aubagnense HPB1.1*
- Metabolites detected: 4-aminophenol, hydroquinone and trans-2-hexenoic acid.
- 50 mg kg^{-1} APAP in sludge were degraded by CSW01 and CSW02 in only 4 days
- Amidases, deaminases, hydroxylases and dioxygenases were involved in APAP degradation

GRAPHICAL ABSTRACT

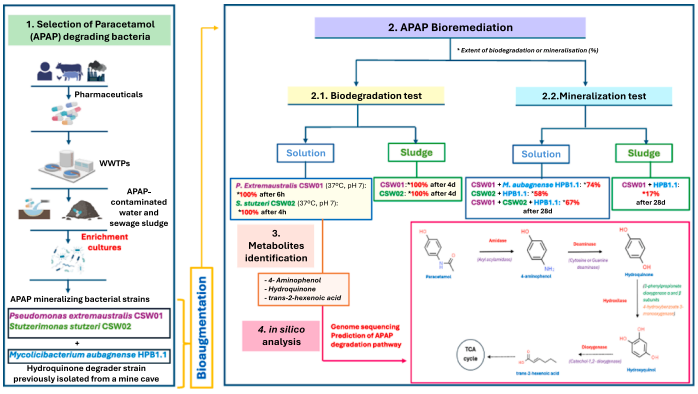

ARTICLE INFO

Keywords:
Paracetamol
Sewage sludge
Pseudomonas extremaustralis
Stutzerimonas stutzeri
Biodegradation
Mineralization

ABSTRACT

Wastewater treatment plants (WWTPs) are recognized as significant contributors of paracetamol (APAP) into the environment due to their limited ability to degrade it. This study used a bioaugmentation strategy with *Pseudomonas extremaustralis* CSW01 and *Stutzerimonas stutzeri* CSW02 to achieve APAP biodegradation in solution in wide ranges of temperature (10–40 °C) and pH (5–9), reaching DT_{50} values < 1.5 h to degrade 500 mg L^{-1} APAP. Bacterial strains also mineralized APAP in solution (<30 %), but when forming consortia with *Mycolicibacterium aubagnense* HPB1.1, mineralization significantly increased (up to 74 % and 58 % for CSW01 +HPB1.1 and CSW02 +HPB1.1, respectively), decreasing DT_{50} values to only 1 and 9 days. Despite the complete degradation of APAP and its high mineralization, residual toxicity throughout the process was observed. Three APAP metabolites were identified (4-aminophenol, hydroquinone and trans-2-hexenoic acid) that quickly disappeared, but residual toxicity remained, indicating the presence of other non-detected intermediates. CSW01 and CSW02 degraded also 100 % APAP (50 mg kg^{-1}) adsorbed on sewage sludge, with DT_{50} values of only 0.7 and 0.3 days,

* Corresponding author.
E-mail address: morillo@irnase.csic.es (E. Morillo).

https://doi.org/10.1016/j.jhazmat.2024.136128
Received 24 April 2024; Received in revised form 8 October 2024; Accepted 8 October 2024
Available online 12 October 2024

respectively, but < 15 % APAP was mineralized. A genome-based analysis of CSW01 and CSW02 revealed that amidases, deaminases, hydroxylases, and dioxygenases enzymes were involved in APAP biodegradation, and a possible metabolic pathway was proposed.

1. Introduction

Pharmaceutical products have been proposed as emerging contaminants of great concern which provokes serious environmental problems due to their potential long-term effects and ecotoxicological risk [1]. One such pollutant that has gained much attention is paracetamol (APAP), a widely used pain reliever. APAP is a common drug found in wastewater mainly coming from households, hospitals effluents and pharmaceutical industries. It is used to treat mild to moderate pain, fever, and inflammation. However, APAP disposed of from household, hospitals or pharmaceutical industries is collected at wastewater treatment plants (WWTPs) where its elimination is not complete, remaining in part in the effluent treated waters (discharged into surface waters used for soil irrigation) and in part adsorbed on sewage sludge (used as fertilizer in agricultural soils). Therefore, APAP is not only detected in surface water, but also in groundwater systems, and tend to accumulate in soil. Despite the low concentration of APAP in these matrices, its presence has been associated with negative effects and toxicity on various species due to its bioaccumulation. Of particular concern is its accumulation in certain aquatic organisms, where it can lead to reproductive, neurotoxic, or endocrine disorders [2-4]. Thus, finding a solution to remove this drug from water and sewage sludge in WWTPs before their release and dispersion into the environment is critical.

One possible solution is the use of bacterial degrading strains in bioaugmentation. Bioaugmentation is a promising approach for improving the biodegradation of pollutants in contaminated environments. This technique involves adding bacterial degrading strains to the contaminated site to enhance the existing microbial population with biodegradation capabilities [5]. The biodegradation of APAP involves the breakdown of the drug into smaller molecules, including mainly formed metabolites 4-aminophenol (4-AP), hydroquinone (HQ), or benzoquinone. These metabolites can be also further broken down by bacteria into less harmful compounds through mineralization. In recent years, only a few bacterial strains have been identified that can degrade APAP. Most of them belong to the *Pseudomonas* genera [6-13], but other genera have shown APAP degradation, such as *Bacillus* [14-16]. Palma et al. [17] isolated eight bacterial strains from two consortia recovered from two marine organisms which exhibited a high APAP removal capacity. *Paenibacillus*, *Micrococcus*, and *Microbacterium* genera were identified as the isolates capable of growing in the presence of 100 mg L^{-1} APAP as the sole carbon source. *Micrococcus yunnanensis* strain TJPT4 showed the highest degrading capacity, reaching 93 % of 15 mg L^{-1} APAP as the sole carbon source after 360 h. Park and Oh [18] isolated *Ensifer sp.* POKHU from activated sludge which degraded up to 630 mg L^{-1} of APAP without substrate inhibition. Two bacterial strains that have shown highly promising results in degrading APAP in solution are those isolated in our group so far [19] designated as *Stutzerimonas stutzeri* CSW02 and *Pseudomonas extremaustralis* CSW01, which showed the ability to degrade 500 mg L^{-1} of APAP in only 6 and 4 h, respectively.

Although bioaugmentation with bacterial degrading strains is a promising approach for treating contaminated environments, several factors need to be considered for its successful implementation, such as strain selection and environmental conditions [20]. Among the various physicochemical parameters that influence bioaugmentation/bioremediation success (chemical structure, concentration and availability of pollutants, nutrients, and oxygen contents, etc.), temperature and pH are especially important. The rate of biodegradation generally increases with temperature, up to a certain point, after which it may decrease or cease completely. Optimal temperatures for biodegradation depend on the specific microorganisms involved and the nature of the organic compound being degraded. In general, mesophilic microorganisms (those that thrive at moderate temperatures, between 20–45 °C) are most commonly used for biodegradation. Higher temperatures can enhance the rate of biodegradation, but if the temperature exceeds the optimal range, it can inhibit microbial growth and activity. On the other hand, lower temperatures can slow down the rate of biodegradation, but the process can still occur, albeit at a slower rate. Similarly, the pH of the environment also plays a crucial role in biodegradation, as it affects the activity of microorganisms involved in the process. The optimal pH range for biodegradation varies also depending on the type of microorganism involved and the organic compound being degraded. In general, most microorganisms thrive at slightly acidic to slightly basic pH levels (pH 6–8). However, some microorganisms can tolerate and even thrive in more acidic or alkaline conditions. If the pH of the environment is outside of the optimal range, microbial activity may be inhibited, leading to slower or incomplete biodegradation. Xagoraraki et al. [21] observed that as pH increased, degradation of APAP also increased when studied in the range of 6–9. Żur et al. [13] determined for *Pseudomonas moorei* KB4 strain, that the optimal pH for APAP degradation was 7, and 30 °C the optimal temperature, whereas Chen et al. [22] reported that the optimal degrading conditions by *Shinella sp.* HZA2 were pH 7.5 and 32.7 °C. Therefore, temperature and pH should be considered alongside other factors when designing and implementing biodegradation processes.

Sewage sludge is an undesirable byproduct of the wastewater treatment process rich in nutrients and organic matter. It is a potential source of energy and fertilizer, but its disposal can be challenging due to its high moisture content, pathogen load, and the presence of toxic organic and inorganic chemicals. Around 1.2 million tonnes of biosolids from WWTPs are produced each year in Spain, and worldwide production will increase to around 150–200 million tons by 2025 [23,24]. Their management and treatment are a major environmental challenge. In developed countries, sewage sludge is treated to produce stable biosolids with agronomic properties rich in organic matter and nutrients (N, P, K, Ca, Mg, and other essential micro-nutrients), adding economic value to what has traditionally been considered a residue [25]. This practice is part of the principles of sustainable management of resources set out in the Circular Economy Action Plan promoted by the EU [26]. Bioaugmentation with bacterial degrading strains is also a potentially viable solution for improving the biodegradation of pollutants in water and sewage sludge from WWTPs. This approach can reduce the environmental impact of pollutants, improving soil and water quality, and protecting public health. However, further research is needed to optimize the technique's effectiveness and to assess its long-term impact on the environment.

Due to the extremely high dispersion of APAP in nature, its environmental fate and ecotoxicological assessment should be a priority [2, 27]. Therefore, the objective of this study is the removal of the APAP and their main formed metabolites to reduce their toxicity in the environment. These chemicals reach different environmental matrices through the use of both effluents and sewage sludge from WWTPs for irrigation and as organic amendments in agricultural soils. The bioremediation technique will be employed through the implementation of a novel technology using bacterial strains to obtain more environmentally friendly biosolids to be used as amendments in agriculture, preventing the contamination of soils and the environment. As previously mentioned, Vargas-Ordóñez et al. [19] showed that *P. extremaustralis* CSW01 and *S. stutzeri* CSW02 were able to biodegrade very high concentrations of APAP in solution as sole carbon and energy source, with a

degradation rate much higher than other APAP-degrader bacterial strains described previously in the literature [6,22,8,18,28,12]. This led us to think about the possible ability of these bacteria to mineralize APAP. In the present study, *S. stutzeri* CSW02 and *P. extremaustralis* CSW01 will be studied under various conditions of pH and temperature to select those most appropriate to carry out APAP biodegradation and mineralization, both in aqueous solution and sewage sludge spiked with APAP. To optimize the mineralization process, these strains were used in conjunction with *Mycolicibacterium aubagnense* HPB1.1, due to the ability of this latter to degrade APAP metabolites that appeared throughout the APAP biodegradation process [29]. Additionally, the feasibility of bioremediation was assessed through ecotoxicity studies to know the toxicity of APAP and its metabolites throughout APAP bioremediation treatments. Finally, the study aimed to characterize the CSW01 and CSW02 strains at the genomic level. The whole-genome sequences were compared to genes of APAP-degrading bacteria obtained from databases and literature to provide new information about the mechanism of APAP biodegradation since genes involved in the APAP degradation pathway are insufficiently understood and seldom investigated.

2. Materials and methods

2.1. Chemicals and materials

The analytical standard of APAP ($C_8H_9NO_2$, N-acetyl-para-aminophenol, CAS 103–90-2, purity $\geq$ 99 %) used in this study was purchased from Sigma-Aldrich (Madrid, Spain) and radiolabelled compound ring-^{14}C-APAP (79.2 mCi mmol^{-1}, 99 % radiochemical purity) was acquired from Hartmann Analytic GMBH (Braunschweig, Germany). Sewage sludge was provided by a WWTP in the city of Seville (Spain) where wastewater treatment included those from a nearby Hospital. The most relevant physicochemical properties of the sludge are described in Table S1 (Supplemental information), with 48 % organic matter and pH 8.25, among other properties. Sewage sludge was used just after being received from the WWTP without any previous treatment to carry out the enrichment cultures with APAP to isolate degrader bacteria. For APAP biodegradation assays in sewage sludge, it was dried at 40° C to constant weight and stored at 4° degrees until use (maximum three months after receiving it).

Mineral salt medium (MSM) used to perform the experiments detailed underneath included principal and essential trace elements (g L^{-1}): 0.5 K_2HPO_4; 0.5 KH_2PO_4; 0.01 NaCl; 0.2 $MgCl_2{\cdot}6H_2O$; 0.02 $CaCl_2$; 0.0004 $ZnSO_4{\cdot}7H_2O$; 0.0004 $CoCl_2{\cdot}6\ H_2O$; 0.0003 $MnSO_4$; 0.01 of EDTA (ethylenediaminetetraacetic acid), 0.0003 $(NH_4)_6Mo_7O_{24}{\cdot}4\ H_2O$ and 1 $(NH_4)_2HPO_4$. All these compounds were purchased from GPR RECTAPUR® (VWR). Luria-Bertani (LB) broth, supplied in dehydrated form by BD Difco™ (Fisher Scientific), was used as culture medium and contained (g L^{-1}): 10.0 tryptone, 5.0 yeast extract, and 10.0 NaCl.

2.2. Bacterial strains

The experiments in this study were performed using bacterial strains *P. extremaustralis* CSW01 and *S. stutzeri* CSW02. Both these bacteria were collected via enrichment cultures of APAP, as previously described by Vargas-Ordoñez et al. [30]. They were selected due to their great degradation capacity for APAP in solution. In addition, a *M. aubagnense* HPB1.1 isolated from mine samples and described as APAP and HQ degrading bacteria by Lara-Moreno et al. [29] was used.

2.3. APAP biodegradation assays in solution under various pH and temperature conditions

Biodegradation experiments of APAP in solution as a sole carbon source were performed in triplicate by inoculating the *P. extremaustralis* CSW01 and *S. stutzeri* CSW02 strains. All materials were sterilized before the assays. 50 mL of MSM sterile solution spiked with APAP (500 mg L^{-1}) was added to 250 mL Erlenmeyer flasks. Sample flasks were inoculated to obtain 10^8 CFU mL^{-1} of the corresponding bacterial strain, whereas control remained without inoculation (to assess a potential abiotic degradation). The bacterial strains were grown in LB medium containing APAP (10 mg L^{-1}) under conditions of 150 rpm agitation at 30 °C and collected at the beginning of the exponential phase. The bacterial pellets were washed twice with MSM solution before the experiment. Growth was monitored using optical density measurements (OD_{600}) on a VWR UV-3100 spectrophotometer, and colony-forming units (CFU) were assessed through serial dilutions plated on LB medium. Each strain was introduced into the degradation experiments at an initial cell density of 10^8 CFU mL^{-1} . Samples were incubated on an orbital shaker at 150 rpm at different conditions of temperature (10, 20, 30, 40 ($\pm$ 1 °C)) and pH (5, 6, 7, 8, 9 ($\pm$ 0.1)) during 20 days (although assays under pH 7 and 30 °C were maintained during 60 days to collect samples for toxicity measurements, as will be explained below). Since the beginning of the experiment, 1 mL samples were periodically sampled (after 1h, 2h, 3h, 4h, 5h, 6h, 7h, 8h, 24h, 30h, 48h, 5d, 10d, 20d) to monitor the APAP concentration remaining in the solution and its possible metabolites produced. To ensure the recovery of APAP present in the supernatant and accumulated in the microbial biomass, samples were subjected to a process of three consecutive cycles of freezing and thawing to break cell walls [31]. Cell suspensions were stored in a freezer during 16–24 h and then thawing the material at room temperature during 8 h. Samples were mixed by vortex before the next cycle. Three cycles were necessary for efficient lysis. Afterward, samples were centrifuged at 11000 rpm for 2 min and supernatant separated for APAP measurement. This process was repeated for every different point of the assay.

2.4. APAP biodegradation assays in sewage sludge

The biodegradation process was also monitored in sludge suspensions. Assays were performed in Corex glass centrifuge tubes containing 500 mg of sludge, spiked with 500 µL of 50 mg L^{-1} APAP solution prepared in methanol, which was evaporated for 24 h in a fume hood to obtain a final concentration of 50 mg kg^{-1}. Afterward, 5 mL of MSM solution was added and inoculated with 10^8 CFU mL^{-1} of bacterial strains in the treatments. Different treatments were carried out: (1) Sterile sludge. Previously autoclaved sludge and MSM solution containing 200 mg L^{-1} of sodium azide to determine the abiotic dissipation of the drug; (2) Sludge. No autoclaved sludge and MSM solution without bioaugmentation with *P. extremaustralis* CSW01 or *S. stutzeri* CSW02 to show the ability of sludge endogenous microbiota to degrade APAP; (3) Sterile sludge + *P. extremaustralis* CSW01 or *S. stutzeri* CSW02; (4) Sludge + *P. extremaustralis* CSW01 or *S. stutzeri* CSW02; (5) Sterile sludge + *P. extremaustralis* CSW01 + *M. aubagnense* HPB1.1; (6) Sludge + *P. extremaustralis* CSW01 + *M. aubagnense* HPB1.1. Inoculation of non-sterilised sludge considers the possible synergies or antagonisms that might exist between the endogenous microbiota and our degrading bacterial strains.

All treatments were equally incubated at 30 °C, pH 7 and 150 rpm during 28 days. At different sampling times (2, 7, 10, 14, 21, 28 d), the corresponding glass tubes were removed and went through a process of freezing and thawing to break the cell walls. APAP content which remained adsorbed in the sludge and dissolved in the supernatant fractions was analysed separately. After centrifugation, 4 mL of the solution were retired for direct analysis by HPLC as described below in Section 2.5. APAP present in the solid phase was extracted using a QuEChERS (Quick, Easy, Cheap, Effective, Rugged & Safe) method: 5 mL of acetonitrile (acidified with 1% acetic acid) were added to the wet residue. The mixture was agitated for 1 min in a vortex mixer. Next, 1 g of a QuEChERS Extract Pouch (Agilent Technologies, reference number 5982–0650) was added, vortexed for another minute, and then centrifuged. The organic phase was separated and cleaned up using 200 mg of

Primary Secondary Amine (PSA, Agilent Technologies). The liquid was decanted, filtered through a 0.45 μm PTFE filter, and analysed by HPLC (as described in Section 2.5). The extraction method had been previously validated in spiked sludge samples, resulting in a recovery of 90–93% of APAP content and a detection limit of 0.05 mg kg^{-1}. The total residual APAP content at each sampling time of the assay was calculated by adding the contents of APAP in the liquid fraction (MSM) and the sludge (QuEChERS extraction) fraction.

2.5. Analytical methods for detection of APAP and metabolites

High-Performance Liquid Chromatography (HPLC) was the technique used to determine the APAP concentration of the supernatant samples. An HPLC coupled to an UV–vis detector (LC-2010AHT, Shimadzu) was used, with a Liquid Purple C-18 column (4×150 mm; Análisis Vínicos, Spain) as stationary phase. Mobile phases consisted of a mixture of methanol and water (10:90 V/V) at pH adjusted to 3 using orthophosphoric acid 85%. The flow was set at 1.1 mL min^{-1}, injection volume was 25 μL and detection wavelength was 244 nm. APAP concentration in sample vials was determined by comparison with calibration curves. In assays of APAP biodegradation in solution, samples were diluted 10-fold, the calibration curve concentration range was 0.1 – 10 mg L^{-1}, with seven calibration points, and correlation coefficient $R^2 > 0.96$. In those assays from biodegradation in sewage sludge, the maximum APAP concentration extracted by ACN from QuEChERS was 10 mg L^{-1}, and the calibration curve used was in the range 0.1 – 10 mg L^{-1}, with seven calibration points, and correlation coefficient $R^2 > 0.99$.

The analysis of APAP-formed metabolites was carried out by liquid chromatography tandem mass spectrometry (LC-MS). The instrument was an Agilent 1290 II Infinity LC system equipment with a vacuum degasser, a binary pump, an autosampler, and a thermostated column compartment (Agilent, USA). Mass spectrometry analysis was carried out on an Agilent 6495c triple-quadrupole-mass spectrometer equipped with an electrospray ionization source. The separation of target compounds was carried out by the injection of 20 μL of sample extract in a Halo C-18 Rapid resolution (50 ×4.6 mm i.d.; 2.7 μm) analytical column (Advanced Materials Technologies, USA) protected by and Halo C18 (5 ×4.6 mm i.d. 4 μm) guard column. Chromatographic analysis was carried out using gradient elution at a flow rate of 0.4 mL min^{-1} using a mobile phase composed of 10 mM ammonium formate (0.05% v/v, formic acid) (solvent A) and acetonitrile (solvent B). Elution started with 2% of solvent B, increased to 5% in 1 min, then to 30% in 3 min and finally to 45% in 4 min. Back to initial conditions was performed in 2 min and held for 4 min for re-equilibration.

The targets APAP metabolites analyzed were: 4-AP, HQ, 1,2,4-trihidroxybenzene, 1,2-dihydroxybenzene, and Trans-2-hexenoic acid. For the ionization of the compounds, the following settings were applied: MS capillary voltage: 3000 V, drying-gas flow rate: 14 L min^{-1}, drying-gas temperature: 200 °C, nebulizer pressure: 20 psi, Fragmentor: 160 V. Each extract was measured using *Multiple Reaction Monitoring* (MRM) mode. At least two transitions were selected for each target compound, except in the case of Trans-2-hexenoic acid. MRM1 was used for the quantification and MRM2 and the ratio were used for confirmation. Conditions applied in MRM mode are shown in Table S2. Calibration curves were constructed by the injection of at least seven calibration standards. Linear range, linearity, limits of detection and quantification, accuracy, and precision of the analytical method are shown in Table S3 (Supplementary material). The analysis of other metabolites whose presence could be suspected, among the previously described in the scientific literature [32,33], was conducted using the same chromatographic conditions applied to the determination of target compounds and mass spectrometry analysis but using Selected Ion Monitoring (SIM) mode. Both positive and negative ionization were applied to the search of potential precursor ions (M+1 and M-1). Subsequently, for the identified parent ions, analysis was performed twice using the Product Ion (PI) mode to identify the MRM transitions of potential APAP metabolites.

2.6. APAP mineralization experiments in solution and sewage sludge

Mineralization studies of ^{14}C-ring-labeled APAP in solution were performed in triplicate, using respirometers, which consist of a modified 100 mL Erlenmeyer flask with a soda tramp, containing 1 mL of 0.5 N NaOH. Erlenmeyer flasks contained 20 mL of MSM, ^{14}C-ring labelled (450 Bq per flask), and unlabelled APAP to obtain a final concentration of 10 or 500 mg L^{-1} in solution. Mineralization studies were conducted as follows:

- In the presence of 10 mg L^{-1}: (1) Control: non-inoculated; (2) *P. extremaustralis* CSW01; (3) *S. stutzeri* CSW02; (4) *M. aubagnense* HPB1.1; (5) *P. extremaustralis* CSW01 + *M. aubagnense* HPB1.1; (6) *S. stutzeri* CSW02 + *M. aubagnense* HPB1.1; (7) *P. extremaustralis* CSW01 + *S. stutzeri* CSW02 + *M. aubagnense* HPB1.1.
- In the presence of 500 mg L^{-1}: (1) Control: non-inoculated; (2) *P. extremaustralis* CSW01; (3) *S. stutzeri* CSW02; (4) *P. extremaustralis* CSW01 + *S. stutzeri* CSW02; (5) *P. extremaustralis* CSW01 + *M. aubagnense* HPB1.1.

The different treatments were inoculated with the volume of the bacterial inoculum necessary to reach an initial concentration of 10^8 CFU mL^{-1}. After inoculating, samples were incubated at 150 rpm and 30 °C during 28 days. The conversion of ring-labelled APAP into $^{14}CO_2$ allowed us to monitor the mineralization of the drug. $^{14}CO_2$ produced was retained using the alkali trap at the top of the flask. Radioactivity was measured by extracting periodically (2–3, 6, 10, 14, 21, 28 days) the NaOH solution and mixing it with 3 mL of a liquid scintillation cocktail (Ready Safe from PerkinElmer, Inc., Waltham, MA, USA). This mixture was stored in darkness for about 24 h to dissipate the chemiluminescence. Radioactivity was evaluated using a liquid scintillation counter (Perkin Elmer Inc., Waltham, MA, USA, Tricarb 4810-TR).

Mineralization assays in sewage sludge slurry were also performed in the same conditions as described in Section 2.4 with the sole difference that 100 mL Erlenmeyer flasks were used instead of Corex Glass tubes. To maintain the proportions mentioned before, sludge was artificially contaminated with a mixture of ^{14}C-APAP (450 Bq per flask) and unlabelled APAP to obtain a concentration of 50 mg kg^{-1}. For that, 2 g of sludge were spiked with 2 mL of 50 mg L^{-1} APAP solution prepared in ethanol, which was then evaporated for 24 h in a fume hood. After evaporation, 20 mL of MSM medium were added to Erlenmeyer flasks and inoculated with 10^8 CFU mL^{-1} of bacterial strains. Samples incubation and measurement took place just as described for assays in solution, with sampling times at 1, 2–3, 4, 7, 14, 21 and 28 days.

2.7. Models of biodegradation and mineralization kinetics

The biodegradation and mineralization kinetics were analysed by fitting curves to the most appropriate kinetic model using an Excel file provided by the FOCUS [34] workgroup on degradation kinetics. The software uses the solver tool from Microsoft's statistical package along with rate curves. Three kinetic models were tested for curve adjustment: a simple first-order model (SFO), a first-order multicompartment model (FOMC), and a biphasic first-order sequential model known as the Hockey-stick (HS) model. The equations for these models are as follows:

$$M_t = M_0 \cdot e^{-kt} \text{ (SFO)}$$

$$DT_{50} = \ln 2/k \text{ (SFO)}$$

$$M_t = M_0/((t/\beta)+1)^{\alpha} \text{ (FOMC)}$$

$$DT_{50} = \beta\,(2\,(1/\alpha) - 1) \text{ (FOMC)}$$

$$\alpha = 1 / (N\text{-}1) \text{ (FOMC)}$$

Table 1
Kinetic parameters calculated from paracetamol (500 mg L^{-1}) biodegradation curves in solution after inoculation with *P. extremaustralis* CSW01 and *S. stutzeri* CSW02 at different temperatures and pH.

Bacterial strain	Temperatures (°C)/pH	Model kinetic	K_1 (h^{-1})	K_2 (h^{-1})	tb	α	β	DT_{50}* (h)	Extent of biodegradation (%)	Calculated χ2 *	Scaled error	R^2
Pseudomonas	10/7	FOMC				108842	1373248	8.7	97.54	5.398	5.24	0.960
extremaustralis	20/7	SFO						3.4	99.99	14.618	7.87	0.935
CSW01	30/7	SFO	0.45					1.5	97.05	13.570	5.72	0.966
	40/7	HS	0.22	0.0018	2.30			190	49.46	11.070	0.66	0.985
Stutzerimonas	10/7	SFO	0.05					14.5	33.34	0.737	2.06	0.938
stutzeri CSW02	20/7	SFO	0.19					3.6	98.85	14.508	8.48	0.915
	30/7	SFO	0.99					0.7	99.97	3.249	0.72	0.999
	40/7	SFO	0.96					0.7	99.95	3.964	0.87	0.999
Pseudomonas	30/5	SFO	0.51					1.4	98.13	13.122	7.88	0.939
extremaustralis	30/6	SFO	0.55					1.3	98.69	12.502	7.60	0.941
CSW01	30/8	SFO	0.56					1.2	98.77	12.505	7.68	0.939
	30/9	SFO	0.45					1.3	98.69	12.101	7.60	0.941
Stutzerimonas	30/5	FOMC				42824	228487	37	37.62	2.095	3.47	0.815
stutzeri CSW02	30/6	SFO	0.59					1.3	98.69	12.111	7.60	0.941
	30/8	SFO	0.56					1.2	97.84	9.885	8.11	0.936
	30/9	SFO	0.59					1.2	98.26	7.999	7.22	0.948

*DT_{50}: time to decline to half the initial concentration of APAP ** χ2 calculated values < χ2 corresponding tabulated value ($p < 0.05$).

$$\beta = (M_0/\ 1\text{-}N) / [k(N\text{-}1)] \text{ (FOMC)}$$

$$Mt = M_0 * e^{(-k1tb)} * e^{(-k2(t-tb))} \text{ (HS)}$$

$$DT_{50} = (\ln 100 / 100 - 50) / k_1 \text{ if } DT_{50} \leq tb \text{ (HS)}$$

$$DT_{50} = tb + (\ln (100 / 100\text{–}50) - k_1\ tb) / k_2 \text{ if } DT_{50} > tb \text{ (HS)}$$

In these equations, M_0 and M_t are the initial APAP concentration and at time t (mg L^{-1}), respectively. DT_{50} denotes the time required for the pollutant concentration to reach half of its initial value. The constant "k" corresponds to the rate of mineralization and biodegradation. In the FOMC model, the parameter α represents the shape, while the parameter β represents the location, the parameter N to calculate α and β corresponds to the number of input compartments. The HS model includes two distinct rate constants for mineralization, "k_1" and "k_2," and "tb," which marks the time at which the rate constant changes. To determine the best-fitted model, the Chi-square (χ^2) test was conducted. This test considers the chi-squared and scaled error values, using the least square of 0.05 as the threshold, to estimate the appropriateness of the model and assess the accuracy of each resulting fit. The selection of these models was based on their relative simplicity, while still having the potential to accurately fit the measured dissipation kinetic datasets for both monophasic and biphasic biodegradation and mineralization [35].

2.8. Ecotoxicity assays

The potential toxicity of the samples before and after of bioremediation experiment in solution was assessed using the Microtox® Test System. This assay employed the bioluminescence of the bacterium *Vibrio fischeri* to measure toxicity, based on the standard protocol using the basic test UNE-EN ISO 11348–3. *V. fischeri* bacterium was rehydrated immediately before use. Assays were conducted in a temperature-controlled photometer at 15 °C (Microbics Corporation (1992). The initial APAP concentration (500 mg L^{-1}) and biodegradation samples at different times were analysed. Before analysis, samples from the APAP biodegradation assays in solution ((1) *P. extremaustralis* CSW01; (2) *S. stutzeri* CSW02; (3) *P. extremaustralis* CSW01 + *M. aubagnense* HPB1.1; (4) *S. stutzeri* CSW02 + *M. aubagnense* HPB1.1) were centrifuged for 10 min to 7000 rpm and serially diluted (1:2) with 2% NaCl solution. The luminescence of samples was measured before adding our bacteria and after inoculation. Samples inoculated with (1) *P. extremaustralis* CSW01, and (2) *S. stutzeri* CSW02 were measured after 2h, 5h, 7h, 1d, 2d, 5d, 10d, 20d, 30d, 45d, and 60d. Samples inoculated with (3) *P. extremaustralis* CSW01 + *M. aubagnense* HPB1.1, and (4) *S. stutzeri* CSW02 + *M. aubagnense* HPB1.1 were measured after 1d, 3d, 5d, 10d, and 20d. The Microtox® Text System provided the EC_{50} parameter, representing the APAP concentration (% v/v) that induced a toxic effect on 50% of the *V. fischeri* population for each sample tested. To quantify the toxicity, the values were converted into toxic units (TU) using the formula $TU = 100/EC_{50}$. The resulting TU values were categorized according to Persoone et al. [36] as follows: $TU < 0.4$: No acute toxicity; $0.4 < TU < 1$: Light acute toxicity; $1 < TU < 10$: Acute toxicity; $10 < TU < 100$: High acute toxicity; $TU > 100$: Very high acute toxicity.

2.9. The genome sequencing data and gene annotation of degrading bacteria

Isolated colonies of *P. extremaustralis* CSW01 and *S. stutzeri* CSW02 were independently transferred to liquid LB medium and cultured overnight. Then, cells were harvested from a 2 mL aliquot by centrifugation (11000 rpm, 2 min) and their DNA was extracted using G-spin™ Total DNA Extraction Kit (iNtRON Biotechnology, Inc). The quality and concentration of DNA were analysed by NanoDrop 2000 (Thermo Fisher Scientific) and horizontal electrophoresis (Sub-Cell GT Cell, BioRad), using 1% (w/v) agarose gel in 1x TAE buffer.

The CSW01 genome was sequenced by Stab Vida company (Caparica, Portugal), using Illumina NovaSeq sequencing data at a coverage of 202x (https://www.stabvida.com/). The generated sequencing reads were assembled using CLC NGS Cell genome assembler version 22.0.1. The CSW02 genome was sequenced by Integrated Microbiome Resource (IMR, Dalhousie University, Canada) using PacBio Sequel2 at coverage from 341x to 351x (https://imr.bio). The generated sequencing reads were assembled using PacBio's SMRTlink genome assembler version 10. The genomes were annotated using the RAST tool (Rapid Annotation Subsystem Technology) and NCBI Prokaryotic Genome Annotation Pipeline. The sequencing data generated in this study has been deposited in the National Center for Biotechnology Information (NCBI). The genome of CSW01 consists of 184 contigs assembled to scaffold level (accessions JAQKGS010000001 to JAQKGS010000184), while the genome of CSW02 consists of three complete genomic sequences (accessions CP140616 to CP140618).

2.10. In silico analysis: nucleotide and protein sequence analysis

Reference protein sequences involved in the APAP biodegradation pathway were sourced from databases and literature and used to search homologs in the genomes of *Pseudomonas extremaustralis CSW01* and

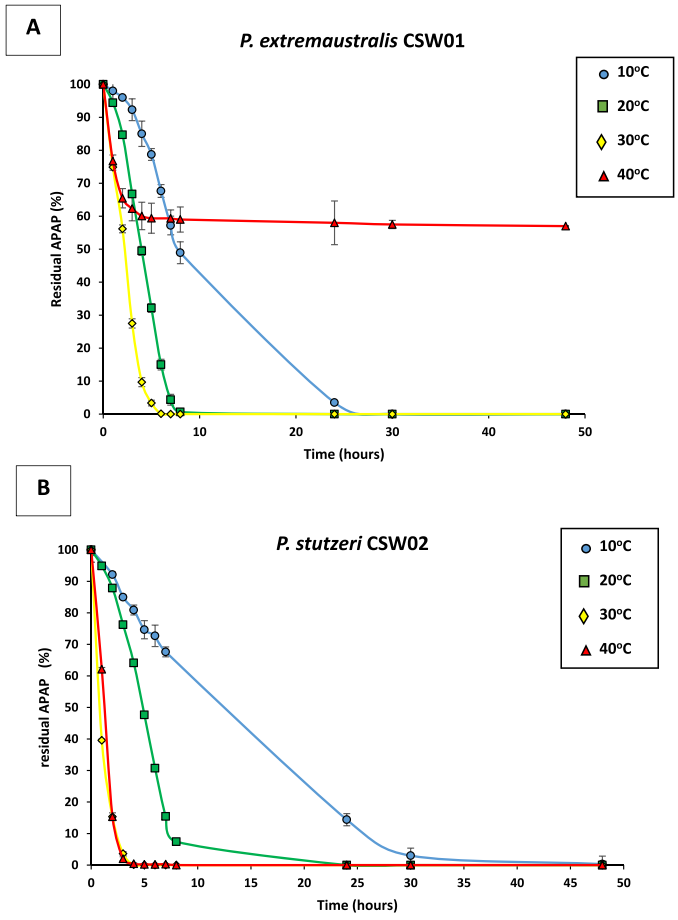

Fig. 1. Paracetamol (500 mg L^{-1}) degradation profiles by *P. extremaustralis* CSW01 (A) and *S. stutzeri* CSW02 (B) under different conditions of temperature.

Stutzerimonas stutzeri CSW02. In the results and discussion section of this subject there is an explanation of the choice of each protein used as a reference. Tblastn (https://blast.ncbi.nlm.nih.gov/Blast.cgi) was used to align these sequences with the genome of the studied bacteria. Default algorithm parameters were employed, with the following settings: Max target sequences: 100, Expect threshold: 0.05, Word size: 5, Max matches in a query range: 0, Matrix: BLOSUM62, Gap costs: Existence: 11, Extension: 1, Compositional adjustments: conditional compositional score matrix adjustment, and Filter: low complexity regions. There is no fixed threshold to determine the precise percentage of identity needed to establish functional. Subsequently, we conducted a study of the catalytic domains of the selected proteins using the Conserved Domain Database (CDD) (https://www.ncbi.nlm.nih.gov/cdd) and InterProScan [37].

3. Results and discussion

3.1. Biodegradation assays in solution under different conditions of temperature and pH

Temperature plays a critical role in the bacterial biodegradation of organic compounds because it influences the growth and metabolism of microorganisms [38,39].

The relationship between temperature and the rate of bacterial biodegradation is well-documented, with higher temperatures generally leading to increased biodegradation rates. This phenomenon can be attributed to the heightened metabolic activity of microorganisms at elevated temperatures, which in turn enhances the diffusion of substrates into the cells, facilitating the biodegradation process [40]. However, there is an optimal temperature range for each microorganism, beyond which the rate of biodegradation may decrease or stop altogether due to the denaturation of enzymes and other cellular components. The maximal biodegradation of xenobiotics seems to occur at the temperature of 30–40 °C [41]. To determine the optimal temperature to carry out the biodegradation of APAP of our bacterial isolates, and that can occur in the environment, the following were tested: 10, 20, 30 and 40 °C (Table 1 and Fig. 1). In the case of *S. stutzeri*, a positively correlated effect of temperature on the degradation of APAP in solution was observed, reducing DT_{50} from 14.5 h for 10 °C to only 0.7 h for 30 and 40 °C. In general, bacteria exposure to low temperatures results in reduced membrane fluidity and low diffusion rates across the membrane, decreasing protein synthesis and protein cold-denaturation and slowing down the kinetics of the cellular processes [42]. On the contrary, in the case of *P. extremaustralis*, a clear trend was observed in the kinetics of APAP degradation, accelerating in the range from 10 to 30 °C (DT_{50} from 8.7 to 1.5 h), but at 40 °C there is a drastic deceleration, with DT_{50} value up to 190 h. This behaviour agrees with the results of López et al. [43] who observed that the growth of this bacterium occurred in a range from 4 to 37 °C, but not at 42 °C, and is consistent with the fact that *P. extremaustralis* is an Antarctic bacterium able to grow under low temperatures [44] which is related to its adaptability to cold environments [45]. Bacteria develop protective adaptation mechanisms in response to very low or very high temperatures, which must be investigated to understand their possible biotechnological applications [40]. As far as we know, only some publications have studied the influence of temperature in APAP biodegradation by bacteria. Most of them indicated that around 30 °C was the optimal temperature [22,15,8]. However, using Design-Expert® software Chopra and Kumar [16] observed that 25 °C gave the best results when using *Bacillus licheniformis* PPY-2 to degrade APAP, and 40 °C when using *Bacillus drentensis* S1 [14].

As well as temperature, pH range is a critical factor influencing the optimal functioning of microorganisms involved in biodegradation processes. While the majority of microorganisms thrive in a neutral pH range of approximately 6.5 to 7, some are capable of tolerating acidic or alkaline environments. For example, fungi generally prefer lower pH levels compared to bacteria. The pH of the surrounding environment directly impacts the ionic charge of microbial cells and the speciation of metal ions, thereby influencing the biodegradation processes and biosorption capabilities of microorganisms. Therefore, changes in pH can affect microbial activity and, consequently, the rate of biodegradation. In particular, the pH may influence the APAP degradation by two different mechanisms: *i*) bacterial strain: pH value may modify both the enzyme structure and substrate affinity. Also, pH can affect the charge of the bacterial cell, which would affect biosorption. At higher pH values surface of the bacterial cells becomes negative, which would lead to changes in electrostatic interaction between the drug and biomass surface. The correlation between biosorption and biodegradation processes has been reported, and changes in pH can influence the biodegradation rate [46]; *ii*) chemical: different pH values determine the chemical speciation of paracetamol. The protonated form (ROH) is present at lower pH and the formation of the phenolate form (RO^-) in an alkaline environment has been observed. However, since pK_a of APAP is 9.5, at neutral and even slightly alkaline pHs APAP is presented mostly in its non-ionic form, and, therefore, its behaviour under the range of pH studied should not be greatly influenced.

When APAP biodegradation assays were performed inoculating *P. extremaustralis* CSW01 at 30 °C in the range of pH from 5 to 9, the kinetic parameters (Table 1) did not show significant differences (DT_{50} from 1.2 to 1.4 h) and APAP was completely degraded in about 4–5 h (Figure S1), indicating that *P. extremaustralis* CSW01 can degrade the pollutant in a broad range of pH. However, in the case of *S. stutzeri* CSW02, although APAP was completely degraded after only 4 h for the pH values 7, 8 and 9, and after 6 h at pH 6, only 25 % APAP could be degraded at pH 5 (Figure S1), even after 48 h′ assay. It seems to indicate that pH 5 is affecting *S. stutzeri* CSW02 microbial cell activity, and the

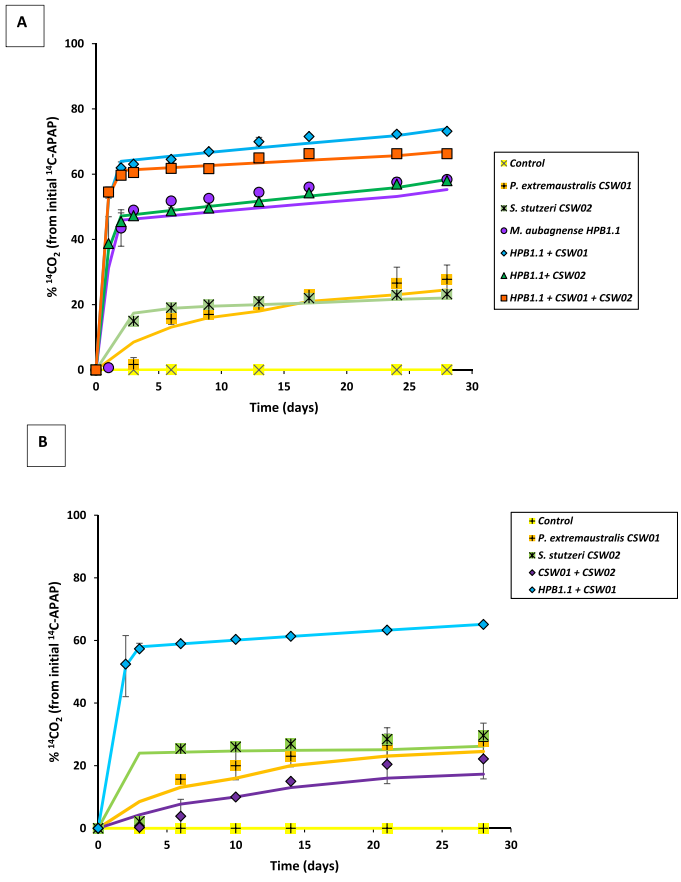

Fig. 2. Paracetamol mineralization in solution A) 10 mg L^{-1} and B) 500 mg L^{-1} after application of different treatments.

range of pH to obtain its maximum degradation is from 6 to 9, also a broad range. Żur et al., [13] carried out a study to determine the optimal pH value for APAP degradation by *P. moorei* KB4 in the range of 4–8, observing a progressive slight increase in APAP degradation up to pH 7, decreasing at pH 8. The same behaviour was also observed by other authors [47,16,8], although, in the case of APAP degradation by *Bacillus pumilus* PYP2, pH 5.0 was the optimum observed [15].

In conclusion, *P. extremaustralis* CSW01 and *S. stutzeri* CSW02, which were very recently described for the first time as APAP-degraders [19], have demonstrated degradation capacity of very high concentrations of this pharmaceutical in wide ranges of both temperature (10–40 °C) and pH (6–9, although CSW01 is also very active at pH 5). It indicates that both bacterial strains are very promising candidates for their use in APAP bioremediation in treatment systems, probably in various environmental conditions.

3.2. APAP mineralization in solution

This study performed mineralization tests using *P. extremaustralis* CSW01 and *S. stutzeri* CSW02 using an APAP concentration of 10 and 500 mg L^{-1}. The environmental conditions selected for the mineralization studies were those previously determined to be the most suitable: pH 7 and 30 °C. Both isolated strains showed mineralization capacity (Fig. 2, Table 2). Similar mineralization capacities after 28 days of assays were observed for both strains and for both concentrations studied, reaching percentages of mineralization extent in the range 23.2–27.6 % for 10 mg L^{-1} APAP concentration and 27.7–29.6 % for 500 mg L^{-1}. The most noteworthy result was the inability of these degrading strains to fully mineralize all the APAP, although, as previously observed,

Table 2
Kinetic parameters calculated from paracetamol mineralisation curves in solution after inoculation with *M. aubagnense* HPB1.1, *P. extremaustralis* CSW01 and *S. stutzeri* CSW02.

APAP concentration (mg L^{-1})	Bacterial strain	Model kinetic	K_1 (day^{-1})	K_2 (day^{-1})	T_b (days)	α (day^{-1})	β (day^{-1})	DT_{50} * (days)	Extent of mineralisation (%)	Calculated χ2 * *	Scaled error	R^2
10	***P. extremaustralis* CSW01**	FMOC	-	-	-	0.105	0.769	1298	27.6	8.21	12.02	0.928
	***S. stutzeri* CSW02**	FMOC	-	-	-	0.045	0.126	∞	23.2	4.32	2.12	0.941
	***M. aubagnense* HPB1.1**	HS	0.373	0.006	1.64	-	-	14	55.3	4.62	5.24	0.807
	CSW01 + HPB1.1	HS	0.739	0.011	1.37	-	-	0.9	73.9	0.53	0.5	0.995
	CSW02 + HPB1.1	HS	0.455	0.008	1.38	-	-	9.0	58.4	0.08	0.23	0.996
	CSW01 + CSW02 + HPB1.1	HS	0.754	0.005	1.25	-	-	0.9	66.9	0.33	0.48	0.996
500	***P. extremaustralis* CSW01**	FMOC	-	-	-	0.098	3.443	4196	27.7	0.62	8.76	0.863
	***S. stutzeri* CSW02**	FMOC	-	-	-	0.078	0.534	3715	29.6	11.07	4.64	0.901
	CSW01 + CSW02	FOMC	-	-	-	0.087	2.681	8003	17.3	8.33	3.48	0.874
	CSW01 + HPB1.1	HS	0.365	0.007	2.4	-	-	1.9	65.2	0.02	0.06	0.999

*DT_{50}: time to decline to half the initial concentration of APAP. * * χ2 calculated values < χ2 corresponding tabulated value (p 0.05).

complete biodegradation of APAP was reached in only 4 and 6 h (Fig. 1). Also, the consortium formed by these two bacteria was proved to mineralize 500 mg L^{-1} APAP, but the result was worse, decreasing the extent of mineralization to 17.3 % (Table 2), likely due to an antagonistic effect between the two bacteria for food sources and territory [48]. Therefore, the observation of limited mineralization capacity by these bacteria leads us to speculate that APAP metabolites should be present in the solution.

To improve APAP mineralization rates, CSW01 and CSW02 were used in conjunction with *M. aubagnense* HPB1.1. This strain has been previously described to be, not only an APAP-degrading bacterium but also capable of degrading its main metabolite, HQ [29]. Fig. 2A shows the APAP mineralization curves for HPB1.1 strain and different combinations of the 3 bacteria used (CSW01 + HPB1.1, CSW02 + HPB1.1, and CSW01 + CSW02 + HPB1.1) for an APAP concentration of 10 mg L^{-1}. In the study with the HPB1.1 strain, the mineralization curve reached 55.3 % APAP mineralization (Table 2), and the kinetic model calculated that 50 % of mineralization (DT_{50}) would be reached after 14 d. A drastic increase in the percentage of mineralization was observed for the mixture of CSW01 + HPB1.1, up to 73.9 % of mineralization, achieving a DT_{50} of only 0.9 days, improving the results obtained with both isolated strains. In the case of CSW02 + HPB1.1 the mineralization results did not improve significantly in comparison to that obtained using only HPB1.1 (58.4 % of mineralization, DT_{50} 9 days). When the three bacterial strains were inoculated forming a consortium, 66.9 % of the extent of mineralization and a DT_{50} of 0.9 days were observed.

Considering mineralization results using a concentration of 10 mg L^{-1}, a higher concentration of 500 mg L^{-1} was tested, using the treatment that yielded the most favorable mineralization results during the 10 mg L^{-1} testing (CSW01 + HPB1.1) (Fig. 2B and Table 2). A significant increase in mineralization extent was also observed, up to 65.2 %, in comparison to inoculation with only CSW01, and a DT_{50} value of only 1.9 days was obtained (Table 2). This mineralization percentage obtained for 500 mg L^{-1} agrees with the data indicated above for low APAP concentration (10 mg L^{-1}). This suggests that the studied degrading consortium can mineralize a wide variety of APAP concentrations. From the results, it can be concluded that the observed improvement in degradation kinetics could be a consequence of the ability of both bacteria to complement each other. On the one hand, CSW01 is highly effective in degrading APAP into HQ, and on the other hand, the mineralization process is enhanced probably thanks to the ability of HPB1.1 to degrade HQ or any other metabolites formed, thereby avoiding its accumulation, and achieving an accelerated process through their combined action.

These results demonstrated the advantages of applying simultaneously two bacterial strains as a biological technique to improve the extent of the mineralization, as well as to accelerate the rate of biodegradation, being the inoculation of *M. aubagnense* HPB1.1 together with *P. extremaustralis* CSW01 the best treatment to restore or reclaim APAP contaminated waters. Bacterial consortia have been previously used to increase the extent of degradation of many organic compounds such as trifluralin [49], diuron [50], polycyclic aromatic hydrocarbons [51] or ibuprofen [52], among others. However, the cooperative mechanism involved in the APAP biodegradation is still unknown. The work carried out by Zhang et al. [12] compared APAP biodegradation using pure bacterial cultures (*Stenotrophomonas* sp. f1, *Pseudomonas* sp. f2 and *Pseudomonas* sp. fg-2) and their bacterial consortium, with different removal efficiency. 2000 mg L^{-1} APAP degraded after 45 h and 60 h, respectively for fg-2 and f2 strains. However, the f1 strain degraded 440 mg L^{-1} of APAP after 116 h. When these strains were combined into a consortium, 4000 mg L^{-1} of APAP was degraded within 37 h. Chopra and Kumar [47] studied the combination of five strains isolated from sewage wastewater, which degraded 1200 mg L^{-1} of APAP in 70 h, whereas individual strains required 10 days for the same task, concluding that the combined microbial culture produced a synergistic impact on the degradation of APAP increasing the rate of the process.

Table 3
Acute toxicity test towards V. fischeri in solution polluted with 500 mg L^{-1} of paracetamol in the presence of *P. extremaustralis* CSW01 or *S. stutzeri* CSW02, and forming consortium with *M. aubagnense* HPB1.1.

Treatment	Time	TU*	SD* *	Toxicity* **
Non-inoculated	0	0.8	0.1	Slight acute toxicity
P. extremaustralis CSW01	2 h	31.5	5.8	High acute toxicity
	5 h	43.0	5.1	High acute toxicity
	7 h	55.3	7.9	High acute toxicity
	1 day	6.7	2.3	Acute toxicity
	2 days	9.1	1.9	Acute toxicity
	5 days	19.9	1.4	High acute toxicity
	10 days	10.0	0.8	High acute toxicity
	20 days	4.5	1.3	Acute toxicity
	30 days	2.7	0.1	Acute toxicity
	45 days	2.6	0.4	Acute toxicity
	60 days	0.2	1.0	No acute toxicity
S. stutzeri CSW02	2 h	22.1	1.4	High acute toxicity
	5 h	17.0	0.4	High acute toxicity
	7 h	10.2	0.3	High acute toxicity
	1 day	10.7	1.7	High acute toxicity
	2 days	10.1	4.2	High acute toxicity
	5 days	16.6	0.9	High acute toxicity
	10 days	12.1	1.4	High acute toxicity
	20 days	4.3	1.8	Acute toxicity
	30 days	3.8	1.1	Acute toxicity
	45 days	3.9	0.4	Acute toxicity
	60 days	3.3	0.6	Acute toxicity
CSW01 + HPB1.1	1 day	130.2	35.7	Very high acute toxicity
	3 days	20.5	11.4	High acute toxicity
	5 days	15.9	9.6	High acute toxicity
	10 days	12.4	3.1	High acute toxicity
	20 days	11.1	1.4	High acute toxicity
CSW02 + HPB1.1	1 day	19.7	7.9	High acute toxicity
	3 days	13.2	8.7	High acute toxicity
	5 days	11.2	6.5	High acute toxicity
	10 days	9.2	2.0	Acute toxicity
	20 days	7.1	3.1	Acute toxicity

*TU: toxic units. * *SD: Standard deviation of three replicates. * ** According to Persoone et al. [36]

Among all bacteria described as APAP degraders, only a few of them have been able to mineralize it. For most of them, mineralization has been deduced by the intermediates produced, especially those metabolites obtained after ring cleavage, but not directly by measuring the amount of CO_2 produced, and therefore the real mineralization rate, as it has been done in the present study. In this sense, Żur et al. [13] observed that the main metabolites formed during APAP degradation by *P. moorei* KB4 included 4-AP, HQ, benzoquinone and p-nitrophenol, and based on the measurements of specific activity of acyl amidohydrolase, deaminase and hydroquinone 1,2-dioxygenase they proposed a mechanism of APAP mineralization by KB4 strain under co-metabolic conditions with glucose. Chopra and Kumar [47] also proposed APAP mineralization by a co-culture of five strains and proposed a new degradation pathway based on new intermediate metabolites detected: 4-AP, HQ, oxalic acid, (R)−2-methylpentanoic acid, 1,5-hexadiene, benzamide, and methylene-3-vinyl cyclohexane, but also ions like –CO, $–NH_2$, nitrates, and nitrites were detected. Chopra and Kumar [14] also proposed that *Bacillus drentensis* S1 mineralized APAP based on the detection of nitrites and nitrates. Also, Chopra and Kumar [15] proposed APAP mineralization by *B. pumilus* PYP2 based on the presence of oxalic acid and formic acid as precursors for CO_2 and H_2O production.

On the contrary, Hu et al. [8] used *Pseudomonas aeruginosa* HJ1012 and observed a CO_2 yield rate up to 71.4 % (similar to the percentage obtained in the present study using the consortia CSW01 +HPB1.1) which proved that the loss of APAP was mainly via mineralization. They identified eight metabolites (4-AP, HQ, formic acid, lactic acid, oxalic acid, succinic acid, nitrate, and nitrite) and proposed two different APAP degradation pathways. Also, Zhang et al. [12] confirmed APAP mineralization based on the total amount of organic carbon (TOC) removals

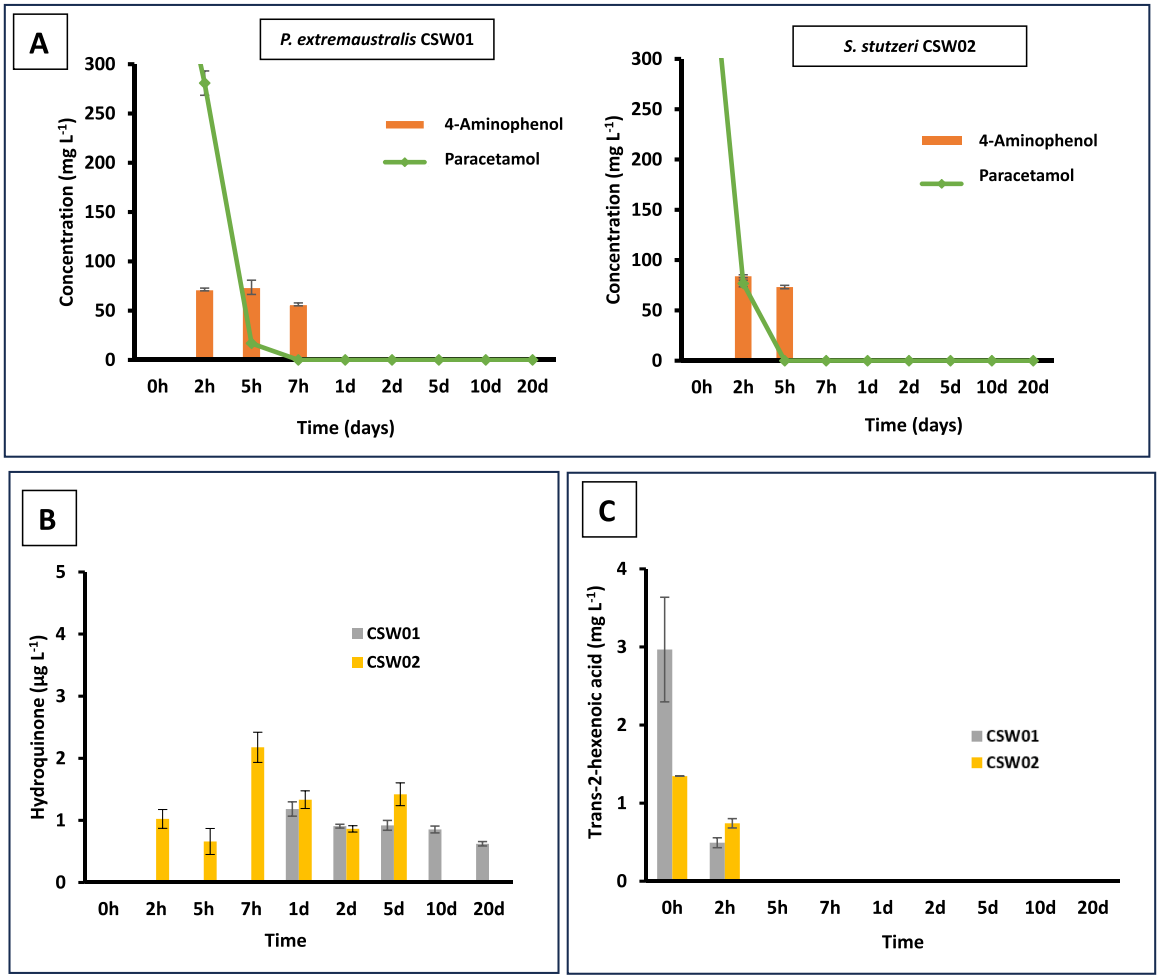

Fig. 3. Concentration of paracetamol metabolites in solution throughout its biodegradation process in the presence of *P. extremaustralis* CSW01 and *S. stutzeri* CSW02. A) Paracetamol and 4-aminophenol; B) Hydroquinone and C) Trans-2-hexanoic acid. Standard deviation (vertical bars).

when using the co-culture of *Stenotrophomonas* f1 strain, and two *Pseudomonas* f2, and fg-2, reaching up to 87.1 %. The metabolites identified include 4-AP, HQ, and some carboxylic and inorganic acids (2-hexenoic acid, succinic acid, malonic acid, oxalic acid, formic acid, nitrate, and nitrite).

Given the scarce number of APAP mineralizing bacterial strains in the literature, it becomes evident importance of *P. extremaustralis* CSW01 and *S. stutzeri* CSW02 and their consortia with *M. aubagnense* HPB1.1 for APAP bioremediation purposes in the environment.

3.3. Ecotoxicity studies in paracetamol-contaminated aqueous samples

We tested the toxicity of non-inoculated APAP solutions (500 mg L^{-1}) and the aqueous samples at different times of APAP degradation in the presence of CSW01 and CSW02 strains (Table 3), and its relation to the presence of APAP metabolites produced throughout the biodegradation process (Fig. 3). The initial concentration of APAP was classified as "Slight acute toxicity" ($0.4 < TU < 1$) according to Persoone et al. [36], with a value of $TU = 0.8$. When bioaugmentation techniques were applied by inoculating CSW01 and CSW02 strains, higher toxicity (>TU values) was observed (Table 3). At 2, 5, and 7 h high acute toxicity was reached indicating the formation of toxic metabolites in the biodegradation process [47]. Three APAP metabolites were detected, 4-AP, HQ and Trans-2-hexenoic acid. This higher toxicity could be due to the presence of 4-AP in the solution at concentrations higher than 50 mg L^{-1} and up to more than 80 mg L^{-1} (Fig. 3A). 4-AP is characterized by mutagenic and teratogenic effects, significant nephrotoxicity, and ability to induce DNA cleavage in human lymphoma cells [39]. However, after only one day of degradation in CSW01 or 7 h in CSW02, 4-AP concentration decreased drastically, with concentrations lower than 200 µg L^{-1} and decreasing with time. Only several bacteria able to degrade 4-AP have been described and CSW01 and CSW02 are two of them. Similar to APAP, 4-AP is poorly biodegradable, being able to inhibit degradation metabolic pathway, slowing down or even stoping the bioremediation processes (Zur et al., 2018a). Also, the metabolite Trans-2-hexenoic acid was detected for both bacterial strains, but fairly early in the experiment (only at 0 h and 2 h), with concentrations in the range 493–2967 µg L^{-1} (Fig. 3C), being completely removed afterward. The presence of Trans-2-hexenoic acid as metabolite was also observed by Zhang et al. [12] and Li et al. [33] and is indicative of the ring fission of APAP aromatic structure. This compound can enter directly into the Krebs cycle leading to mineralization. Despite the very low concentrations of 4-AP and the absence of Trans-2-hexenoic acid, acute toxicity or even high acute toxicity remained. The presence of another APAP metabolite such as HQ (Fig. 3B) was also observed, and in this case, it remained until day 20 for CSW01 and day 5 for CSW02 (Fig. 3B), but at a much lower concentration (below 2 µg L^{-1}), which was maintained more or less constant. APAP can be degraded to HQ directly or via 4-AP as a metabolic intermediate [18]. HQ is known to be a transient metabolite [17], and this is the reason for the extremely low concentrations observed since it is degraded very quickly.

Despite the low concentrations of 4-AP after 5–7 h of inoculation and

the extremely low concentrations of HQ, toxicity was maintained mainly as "high acute toxicity" until day 10, after which it remained as "acute toxicity" until day 45 for CSW01 and day 60 for CSW02. It indicates that, although APAP had disappeared from solution in only 4–6 h when bioaugmented with CSW01 or CSW02, the presence of other toxic metabolites produced throughout the process and that remained for almost two months must be a certainty. However, no more metabolites were detected with the analytical method used.

The toxicity concentration of APAP for *Escherichia coli* demonstrated that its minimum inhibitory concentration (MIC) was 2.5 g L^{-1} [53], higher than 1.75 g L^{-1} for 4-AP [54], and much higher than only 0.26 g L^{-1} for HQ [55]. Park and Oh [18] also observed that 4-AP and HQ inhibit nitrogen metabolism (ammonium oxidation) of microbial communities to a greater extent than APAP, suggesting the higher toxicity of these APAP metabolites. To know if the metabolites detected in this study, 4-AP and HQ were responsible for the toxicity observed, pure solutions of 4-AP and HQ were subjected also to ecotoxicity measurements by Microtox (data not shown). The results obtained indicated that a 4-AP concentration of 10 mg L^{-1} presented a TU value of 9.97 (1 <TU<10, acute toxicity), but a 4-AP concentration of 1 mg L^{-1} was not toxic (TU <0.1). It indicates that 4-AP values > 50 mg L^{-1} measured in CSW01 and CSW02 in Fig. 3A could be responsible for the toxicity observed. In the case of HQ, a concentration of 100 μg L^{-1} presented a TU value of 3.88 (acute toxicity), but concentrations of 10 and 1 μg L^{-1} presented TU values < 0.4 (no acute toxicity), indicating that the concentrations of HQ measured, which were in almost all cases < 2 μg L^{-1} (Fig. 3B), were not the responsible of the toxicity in those samples where 4-AP was not present. The results of the ecotoxicity test indicate that there must be a continuous formation of toxic metabolites throughout APAP biodegradation process, most of them not detected by the analytical method used in this work, which are even more toxic than the parent compound [56].

Toxicity analysis of the samples was also conducted when *M. aubagnense* HPB1.1 was inoculated simultaneously with CSW01 or CSW02 (Table 3), and the toxicity values were similar to those observed when both strains were inoculated alone. The metabolites detected were also similar (Figure S2), but in the case of 4-AP the concentrations detected were lower (Fig. 3SA), and in the case of CSW01 + HPB1.1 the drastic decrease of its concentration occurred much later, remaining in solution until day 3. Also, HQ concentrations detected were quite similar to those obtained with only CSW01 or CSW02 (Figure S2B). Similarly, Trans-2-hexenoic acid was detected (Figure S2C), but very early in the treatment process in the case of the consortium CSW02 + HPB1.1 (1265 μg L^{-1} at day 0), while for CSW01 + HPB1.1 it remained until day 1 with 1058 μg L^{1}. In the present study, despite observing high percentages of mineralization after 28 days of the inoculation with both consortia (73.9 % % and 58.4 % for CSW01 + HPB1.1 and CSW02 + HPB1.1, respectively), elevated levels of toxicity were still observed, likely due to the presence of other not detected metabolites. The presence of 4-AP and HQ as the main APAP metabolites has been shown by several authors [8,57,58,13], which have reported also the formation of highly toxic intermediates derived from APAP distinct from HQ and 4-AP. In the presence of microorganisms in soil, Li et al. [33] identified eight aromatic intermediates from APAP biodegradation, including 3-hydroxyacetaminophen, HQ, and 1,4-benzoquinone. Chopra and Kumar [47] identified benzamide, (R)−2-methylpentanoic acid, methylene-3-vinyl cyclohexane, and 1,5-hexadiene as relevant intermediate metabolites in the APAP biodegradation test. According to the metabolites detected, various APAP biodegradation pathways have been described [39].

In conclusion, previous results show that assessing target contaminant levels through analytical techniques remains crucial for the implementation of bioremediation treatments, but merely observing a decline in the target pollutant concentration is not sufficient to confirm a decrease in toxicity. This is due to the potential presence of toxic metabolites resulting from the biodegradation process, as highlighted by previous studies [59,60].

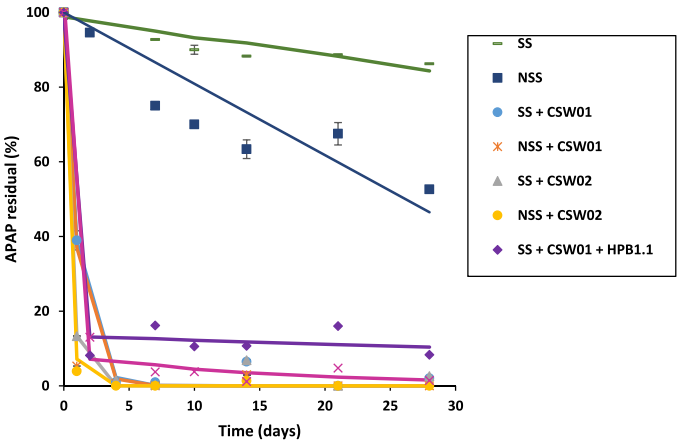

Fig. 4. Biodegradation curves of paracetamol in sterile (SS) and non-sterile sewage sludge (NSS) without treatments, and in the presence of CSW01, CSW02, and HPB1.1 strains. Vertical lines show standard deviation.

3.4. APAP biodegradation in sewage sludge

One aim of this study was to diminish the levels of APAP and its metabolites, not only in solution but also in samples of sewage sludge, to produce environmentally friendlier biosolids. Consequently, the effectiveness of the individual degrading bacterial strains CSW01 and CSW02, as well as the combined strains CSW01 + HPB1.1, which demonstrated the highest APAP mineralization efficiency in solution, was evaluated in sewage sludge. The goal of this assay was to reduce the concentration of APAP in sewage sludge suspensions that were deliberately contaminated with this pollutant. Fig. 4 illustrates the percentages of remaining APAP in the slurry system (the sum of what is present in the solid and the aqueous phases) under the various treatments, and the corresponding kinetic parameters are shown in Table 4.

The assay using sterilized sludge (SS) (Fig. 4) demonstrated the abiotic dissipation of APAP in the sludge after treatment with sodium azide to eliminate any biotic effect. A significant dissipation was observed (15.7 % after 28 days). This means that abiotic factors have to be taken into account as partially responsible for the degradation or transformation achieved with the different treatments. Several authors describe abiotic factors as responsible for the removal of paracetamol from the environment. Palma et al. [61] observed the presence of HQ and 4-AP in the abiotic control of APAP biodegradation tests. This study justifies their presence due to the hydrolysis of APAP, which is accelerated by the presence of oxygen. Also, a partially irreversible adsorption of APAP on sludge, which could be increased with time, could be occurring. In this system SS and also in the *unsterilized sludge* control without bacterial inoculum (NSS), only about 37 % of APAP previously adsorbed on sewage sludge was transferred to the aqueous phase when 5 mL of MSM solution was added to 0.5 g sludge to obtain the slurry. The rest of APAP remained adsorbed.

In NSS, a higher APAP dissipation was observed (50.3 % after 28 days) compared to the sterile control (SS). From this result, it was concluded that, in addition to abiotic dissipation, the endogenous microbiota of the sludge harbors microorganisms capable of utilizing APAP as a carbon source.

When the CSW01 and CSW02 strains were individually inoculated in both, SS and NSS, a complete APAP degradation was observed after only 4–7 days (Fig. 4). Additionally, the DT_{50} was significantly reduced to less than 1 day compared to 122 and 31 days for SS and NSS, respectively (Table 4). These results indicate that both bacterial strains can fully degrade APAP, not only in solution but also when it is adsorbed onto sludge. It is worth noting that the bacterial strains studied in this

Table 4
Kinetic parameters calculated from paracetamol (50 mg Kg^{-1}) biodegradation curves in a water-sludge system after inoculation with *M. aubagnense* HPB1.1, *P. extremaustralis* CSW01 and *S. stutzeri* CSW02.

Bacterial strain	Model kinetic	K_1 (day^{-1})	K_2 (day^{-1})	T_b (h)	DT_{50} * (days)	Extent of biodegradation (%)	Calculated $\chi 2$ * *	Scaled error	R^2
SS	SFO	0.006	-	-	122	15.7	0.299	1.71	0.849
SS + CSW01	SFO	0.950	-	-	0.7	100	6.148	0.46	0.999
SS + CSW02	SFO	2.017	-	-	0.3	100	5.098	0.36	0.999
SS + CSW01 + HPB1.1	HS	1.471	0009	1.37	0.5	91.7	5.822	1.04	0.979
NSS	SFO	0.022	-	-	30.7	50.3	5.683	6.73	0.763
NSS + CSW01	SFO	0.997	-	-	0.7	100	0.839	0.36	0.997
NSS + CSW02	SFO	2.636	-	-	0.3	100	0.002	0	0.999
NSS + CSW01 + HPB1.1	HS	1.687	0.058	1.57	0.4	98.6	9.834	0.83	0.993

* DT_{50}: time to decline to half the initial concentration of APAP. * * $\chi 2$ calculated values < $\chi 2$ corresponding tabulated value (p 0.05).

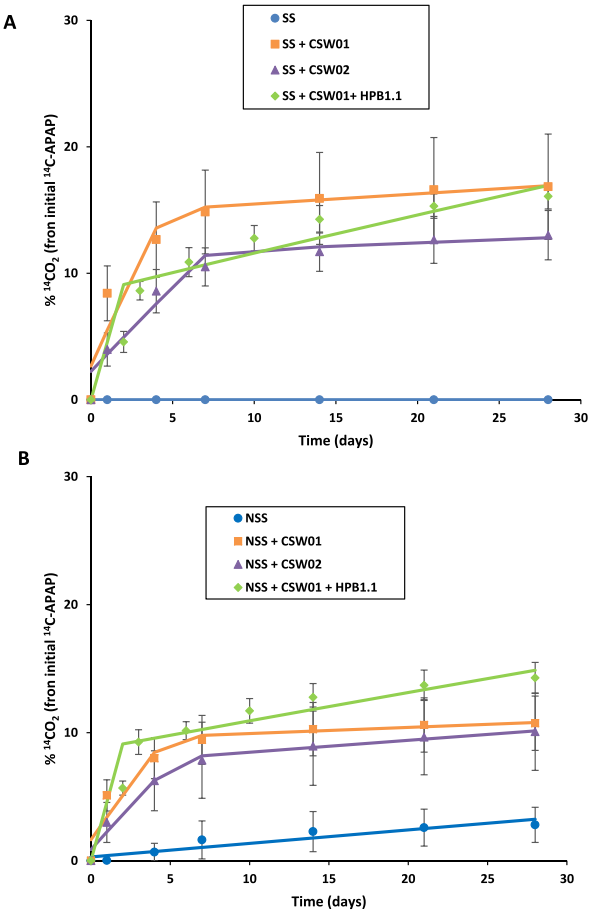

Fig. 5. Paracetamol mineralization in sewage sludge (50 mg Kg^{-1}) after application of different treatments: A) Sterilized Sludge (SS); B) Non-Sterilized Sludge (NSS).

work had never been previously described in the literature as APAP degraders in biodegradation studies in sludge. As far as we know, this is the first study dealing with the degradation of pharmaceuticals from sludge through bioaugmentation using isolated bacteria. Only the studies of Liu et al. [62] and Aguilar-Romero et al. [52] demonstrated the degradation of gentamicin and ibuprofen, respectively, but using bacterial consortia.

Finally, the degrading capacity of the CSW01 bacterium alongside HPB1.1 was tested in both sterile and non-sterile sludge. This selection was based on the mineralization results in solution, where CSW01 + HPB1.1 achieved the highest mineralization percentage (Fig. 2). The results showed very similar outcomes to when CSW01 was inoculated individually: 91.7 % and 98.6 % APAP biodegradation (slightly lower), with DT_{50} of 0.5 and 0.4 days in SS and NSS, respectively (Fig. 4 and Table 4). Based on these findings, it is concluded that the complete biodegradation of APAP in sludge does not require the combination of the studied strains forming consortia with other degrading bacteria.

3.5. APAP mineralization in sewage sludge

Fig. 5 and Table 5 show the APAP mineralization curves and the corresponding kinetic parameters obtained after the application of different treatments in sterilized sludge (SS) and non-sterilized sludge (NSS). As expected, APAP mineralization in SS was not observed in this study (Fig. 5A), whereas the effect of natural attenuation by the presence of endogenous microbiota using NSS (Fig. 5B) showed a minimal APAP mineralization (3.2 %, Table 5). An increase in mineralization to 16.9 % and 10.8 % after 28 days for SS and NSS, respectively, was observed when the CSW01 strain was inoculated, and similar results were obtained when the CSW02 strain was incorporated into the SS or NSS, in which 12.8 % and 10.1 % of APAP mineralization were achieved, respectively. Despite improving the mineralization process when the isolates CSW01 and CSW02 were used for inoculation, the previous results of APAP mineralization in solution suggest the need to resort to the combination of the CSW01 and HPB1.1 strains forming a consortium. Compared to the previously discussed treatments, the addition of CSW01 + HPB1.1 did not increase the percentage of mineralization for SS (16.9 %) and only a slight increase up to 14.9 % for NSS. Data about the required time to achieve 50 % mineralization given by the kinetic model are not useful in these cases where only mineralization below 17 % was obtained.

The results obtained indicate that, although the percentages of APAP mineralization in solution drastically increased when CSW01 formed a consortium with HPB1.1 (from 27.6 % to 73.9 % for APAP 10 mg L^{-1}, and from 24.5 % to 65.2 % for 500 mg L^{-1}), the same is not observed when this consortium is applied in sewage sludge contaminated with APAP, with a value up to only 16.9 % APAP mineralized. It could indicate that the presence of the sludge prevents CSW01, CSW02 and the consortia CSW01 + HPB1.1 from exercising their mineralizing power demonstrated in solution. Such behaviour is not due to competence with endogenous microbiota because the same effect was also observed when the sludge was sterilized (SS) (Table 5).

On the other hand, this low mineralization value (only 16.9 %) also contrasts with those obtained for APAP biodegradation in sewage sludge using CSW01 (100 % APAP biodegraded) and the consortium CSW01 + HPB1.1 (98.6 % APAP biodegraded). In summary, although a complete APAP biodegradation was achieved in sewage sludge, only limited mineralization was observed. It could indicate that the metabolites produced due to the biodegradation process could be more hydrophobic than APAP, remaining adsorbed on the sludge, and reducing their bioavailability to be mineralized. But this possibility does not seem to be the reason, because 4-AP and hydroquinone are highly soluble in water (16 and 72 g L^{-1}, respectively) and their log Kow values are also

Table 5
Kinetic parameters calculated from paracetamol (50 mg kg^{-1}) mineralization curves in a water-sludge system after inoculation with *M. aubagnense* HPB1.1, *P. extremaustralis* CSW01 and *S. stutzeri* CSW02.

Bacterial strain	kinetic Model	K_1 (day^{-1})	K_2 (day^{-1})	Tb (days)	DT_{50} * (days)	Extent of mineralization (%)	Calculated $\chi 2$ * *	Scaled error	R^2
Sterilized sludge (SS)	SFO	0.0001	-	-	∞	0	0.002	1.25	0.991
SS + CSW01	HS	0.029	0.001	4.6	583	16.9	0.174	0.26	0.927
SS + CSW02	HS	0.014	0.001	5.4	1020	12.8	0.075	0.17	0.958
SS + CSW01 + HPB1.1	HS	0.145	0.003	0.9	159	16.9	0.558	0.78	0.839
Non Sterilized sludge (NSS)	SFO	0.001	-	-	647	3.24	0.0008	0.30	0.881
NSS + CSW01	HS	0.018	0.001	4.7	1140	10.8	0.061	0.15	0.9369
NSS + CSW02	HS	0.013	0.001	7.3	610	10.1	0.014	0.07	0.983
NSS + CSW01 + HPB1.1	HS	0.247	0002	0.5	225	14.9	0.275	0.53	0.891

*DT_{50}: time to decline to half the initial concentration of APAP. * * $\chi 2$ calculated values < $\chi 2$ corresponding tabulated value (p 0.05).

low (−0.09, 4-AP; 0.59, HQ), indicating these compounds do not have a high potential for adsorption to sewage sludge. It seems to indicate again that, as in the results obtained in toxicity studies, other metabolites not detected with the analytical method used in this study must be present, and these could be more hydrophobic than APAP and the metabolites detected. The adsorption on sludge of these more hydrophobic metabolites could prevent further mineralization. Despite this, the fact that a complete biodegradation of 50 mg kg^{-1} APAP in sewage sludge has been reached is a magnificent result, although the presence of certain APAP metabolites in sludge must be considered.

3.6. *In silico analysis of genes involved in paracetamol degradation pathway*

In this work, an *in silico* study of the bacteria *P.extramaustralis* CSW01 and *S. stutzeri* CSW02 has been carried out to identify genes potentially involved in the degradation pathway of APAP. This study provides valuable genetic information in the field of bioremediation, by offering a deeper understanding of the microbial mechanisms involved in the biodegradation/mineralization of APAP. In the case of *M. aubagnese* HPB1.1, a complete analysis of the protein involved in the APAP biodegradation pathway was conducted by Lara-Moreno et al. [29].

The *P. extramaustralis* CSW01 and *S. stutzeri* CSW02 genomes are composed of 184 and 3 contigs for a total of 7056,049 bp and 5025,868 bp and 60.1 % and 63,5 % of G + C content, respectively. A total of 6584 coding sequences were identified in the genome of CSW01. Moreover, one 16 s rRNAs, two 5 s rRNAs, one 23 s rRNAs, and 56 tRNAs were found. In the case of the CSW02 strain, 4806 coding sequences were identified, including four 16S rRNAs, four 5S rRNAs, four 23S rRNAs, and 60 tRNAs.

For a general characterization of the potential of the strains to degrade persistent organic compounds, the metabolism of aromatic compounds was seen in more detail. Interestingly, the CSW01 and CSW02 genomes contain 66 and 75 genes related to the metabolism of aromatic compounds, respectively (Fig. 3S, boxed in red). These genes have been classified into different subsystems: (1) peripheral pathways for catabolism of aromatic compounds, (2) metabolism of central aromatic intermediates, and (3) metabolism of aromatic compounds - no subcategory. 38 genes in the case of CSW01 strain and 45 genes for CSW02 were classified within the peripheral subsystems. They are involved in the degradation of salicylate, phenol, biphenyl, quinate, n-Phenylalkanoic acid, benzoate, and p-Hydroxybenzoate. Conversely, 23 genes for CSW01 and 28 genes for CSW02 are responsible for the metabolism of central aromatic intermediates, such as the catechol and protocatechuate branch of the beta-ketoadipate pathway, salicylate and gentisate catabolism, and homogentisate pathway. Finaly, 5 and 2 genes were identified for CSW01 and CSW02 strains, respectively, related to the degradation of gentisate.

Furthermore, even if some enzymes responsible for the above-mentioned pathways have been reported in the APAP degradation pathway [63], an additional search was carried out following another strategy to specifically identify *P. extremaustralis* CSW01 and *S. stutzeri* CSW02 genes potentially involved in APAP degradation. Genes potentially associated with APAP biodegradation were *in silico* predicted in the genomes of these strains by analyzing the sequence homology of their encoded proteins with enzymes having a role in the APAP degradation pathway described by Ríos-Miguel et al. (2022), thus considered reference proteins in this *in silico* search strategy. The homologous proteins putatively involved in the APAP biodegradation identified in the CSW01 and CSW02 genomes are listed according to the hypothesized metabolic pathway in Tables 6 and 7, respectively.

Typically, the required level of similarity to confirm that two proteins in different bacteria share the same function can vary based on several factors, such as the degree of conservation at the protein level and the specific functional regions involved. There is no fixed threshold to determine the precise percentage of identity needed to establish functional equivalence. However, in general, a higher level of similarity suggests a greater likelihood of functional resemblance between the proteins. According to Rost [64], sequence alignments can reliably differentiate between pairs of proteins with similar and dissimilar structures when the sequence identity is high (above 40 % for lengthy alignments). Also, Todd et al. [65] investigated the variation in enzyme function among different superfamilies and concluded that, in the case of both single and multi-domain proteins, there is minimal variation in the Enzyme Commission (EC) number (a number associated with a specific enzyme-catalyzed reaction) when the sequence identity exceeds 40 %. Thus, if the sequence identity surpasses this threshold, it is highly likely that the proteins retain the same function. Nevertheless, the percentage of identity between proteins might be below 40 % due to evolutionary divergence but maintain similar functions. Indeed, Rost [64] reported that there is an ambiguous zone (30 % to 35 % similarity) described by an explosion of false negatives, and above a cut-off of 30 % identity about 90 % of the detected pairs were homologous. This clearly shows the considerable diversity of homolog proteins across organisms, highlighting the interest in searching for new homologs.

Based on Ríos-Miguel et al. [66], amidases are responsible for the first APAP biodegradation step by transforming APAP into 4-AP. Four amidases reported as able to transform APAP to 4-AP or to a brown compound (aryl acylamidase described for Bacterium CSBL00001, Accession number: ACP39716.2 [67]; aryl-amidase A described for *Paracoccus huijuniae* FLN-7, Accession number: AFC37599.1 [68]; aryl-amidase described for *Ochrobactrum* sp. PP-2, Accession number: ANS81375.1 [69]; aryl-amidase described for *Rhizorhabdus wittichii* DC-6, Accession number: AGC74206.1 [70] were used as references to search for homologsand, in the *P. extremaustralis* CSW01 and *S. stutzeri* CSW02 genomes and significant alignments were found with all of them (thresholds described in the Materials and Methods section). Each found amidase showed an identity percentage greater than 30 % with the respective reference protein (described in the literature) (Tables 6 and 7, respectively). Interestingly, the protein described for Bacterium CSBL00001 reached an identity percentage of 85 % to proteins encoded in both the target genomes (CSW01 and CSW02), which shows very

Table 6
Information about the alignment of amidase, deaminases, hydroxylase, and dioxygenase proteins, known to degrade paracetamol and proteins annotated in the genome of *P. extremaustralis* CSW01.

	REFERENCE PROTEIN DATA			ALIGNMENT DATA			ANNOTATE PROTEIN DATA		
	Protein (Accession number)	Function	Bacterium	Coverage (%)	Identity (%)	E-value	Contig	Peg annotation	Putative function
Amidases	ACP39716.2	aryl acylamidase	Bacterium CSBL00001	98	85	0	2	1844	*Hypothetical protein
	AFC37599.1	aryl-amidase A	*Paracoccus huijuniae* FLN-7	94	31	$4e^{-28}$	52	4635	Aspartyl-tRNA(Asn) amidotransferase subunit A
	ANS81375.1	aryl-amidase	*Ochrobactrum* sp. PP-2	99	47	$7e^{-137}$	2	1844	Hypothetical protein
	AGC74206.1	aryl-amidase	*Rhizorhabdus wittichii* DC-6	69	36	$3e^{-37}$	8	6263	Acetylpolyamine aminohydrolase
Deaminases	WP_130204088.1	Cytosine deaminase	*Pseudomonas* sp. MIL9	92	30	$4e^{-36}$	71	5738	*Cytosine deaminase
	WP_147428858.1	Guanine deaminase	*Paracoccus* sp. APAP_BH8	98	53	$4e^{-146}$	41	3865	*Guanine deaminase
Hydroxilases	AKA64675.2	aromatic-ring-hydroxylating oxygenase alpha subunit	uncultured bacterium	89	28	$2e^{-39}$	2	1868	3-phenylpropionate dioxygenase alpha subunit
	AYA78733.1	aromatic-ring-hydroxylating oxygenase beta subunit	uncultured bacterium	87	32	$2e^{-10}$	2	1867	hypothetical protein
	WP_024845849.1	4-hydroxybenzoate 3-monooxygenase	*Paracoccus* sp. APAP_BH8	100	54	$1e^{-134}$	34	2986	*P-hydroxybenzoate hydroxylase
Dioxygenases	AEH41576.1	hydroquinone dioxygenase large subunit	*Sphingomonas* sp. TTNP3	-	-	-	-	-	No significant similarity
	ABU50916.1	hydroquinone dioxygenase large subunit	*Pseudomonas* sp. WBC-3	-	-	-	-	-	No significant similarity
	ABU50916.1	hydroquinone dioxygenase small subunit	*Pseudomonas* sp. WBC-3	-	-	-	-	-	No significant similarity
	KAB7760265.1	extradiol ring-cleavage dioxygenase III subunit A	*Mycolicibacterium mucogenicum* DSM 44124	39	27	$2e^{-07}$	24	2102	Succinate dehydrogenase/fumarate reductase, flavoprotein subunit
	KAB7760264.1	extradiol ring-cleavage dioxygenase III subunit B	*Mycolicibacterium mucogenicum* DSM 44124	95	38	$1e^{-42}$	82	6359	Hypothetical protein
	ANH99603.1	intradiol ring-cleavage dioxygenase	*Pseudomonas koreensis* CRS05-R5	98	41	$31e^{-66}$	2	1865	*Catechol 1,2-dioxygenase
	BAN53997.1	hydroxyquinol 1,2-dioxygenase	*Pseudomonas putida* NBRC 14164	98	41	$7e^{-67}$	2	1865	*Catechol 1,2-dioxygenase

- * Candidate proteins most likely to be responsible for APAP biodegradation based on identity and coverage percentage (respective gene sequences are reported in Supplementary material S5).
- Peg (Protein Encoding Gene) from RAST server.

Table 7
Information about the alignment of amidase, deaminases, hydroxylase, and dioxygenase proteins, known to degrade paracetamol and proteins annotated in the genome of *S. stutzeri* CSW02.

	REFERENCE PROTEIN DATA			ALIGNMENT DATA			ANNOTATE PROTEIN DATA		
	Protein (Accession number)	Function	Bacterium	Coverage (%)	Identity (%)	E-value	Contig	Peg annotation	Putative function
Amidases	ACP39716.2	aryl acylamidase	Bacterium CSBL00001	98	85	0	33	4530	*Hypothetical protein
	AFC37599.1	aryl-amidase A	*Paracoccus huijuniae* FLN-7	94	31	$4e^{-28}$	23	1786	Aspartyl-tRNA(Asn) amidotransferase subunit A
	ANS81375.1	aryl-amidase	*Ochrobactrum* sp. PP-2	99	47	$7e^{-137}$	33	4530	Hypothetical protein
	AGC74206.1	aryl-amidase	*Rhizorhabdus wittichii* DC-6	55	30	$2e^{-14}$	23	1648	Deacetylases
Deaminases	WP_130204088.1	Cytosine deaminase	*Pseudomonas* sp. MIL9	89	30	$3e^{-30}$	23	186	*Cytosine deaminase
	WP_147428858.1	Guanine deaminase	*Paracoccus* sp. APAP_BH8	97	54	$4e^{-142}$	23	4001	*Guanine deaminase
Hydroxilases	AKA64675.2	aromatic-ring-hydroxylating oxygenase alpha subunit	uncultured bacterium	80	30	$5e^{-43}$	23	2446	*Benzoate 1,2-dioxygenase alpha subunit
	AYA78733.1	aromatic-ring-hydroxylating oxygenase beta subunit	uncultured bacterium	87	32	$1e^{-10}$	23	4553	*hypothetical protein
	WP_024845849.1	4-hydroxybenzoate 3-monooxygenase	*Paracoccus* sp. APAP_BH8	-	-	-	-	-	No significant similarity
Dioxygenases	AEH41576.1	hydroquinone dioxygenase large subunit	*Sphingomonas* sp. TTNP3	-	-	-	-	-	No significant similarity
	ABU50916.1	hydroquinone dioxygenase large subunit	*Pseudomonas* sp. WBC-3	-	-	-	-	-	No significant similarity
	ABU50916.1	hydroquinone dioxygenase small subunit	*Pseudomonas* sp. WBC-3	-	-	-	-	-	No significant similarity
	KAB7760265.1	extradiol ring-cleavage dioxygenase III subunit A	*Mycolicibacterium mucogenicum* DSM 44124	82	27	$2e^{-67}$	23	3059	Succinate dehydrogenase/fumarate reductase, flavoprotein subunit
	KAB7760264.1	extradiol ring-cleavage dioxygenase III subunit B	*Mycolicibacterium mucogenicum* DSM 44124	63	40	$7e^{-30}$	23	2967	Hypothetical protein
	ANH99603.1	intradiol ring-cleavage dioxygenase	*Pseudomonas koreensis* CRS05-R5	50	25	$3e^{-05}$	23	2453	Catechol 1,2-dioxygenase
	BAN53997.1	hydroxyquinol 1,2-dioxygenase	*Pseudomonas putida* NBRC 14164	98	41	$7e^{-67}$	23	2453	*Catechol 1,2-dioxygenase

- * Candidate proteins most likely to be responsible for APAP biodegradation based on identity and coverage percentage (respective gene sequences are reported in Supplementary material S5).
- Peg (Protein Encoding Gene) from RAST server.

strong evidence of homology, and Ko et al. [71] have proved, through overexpression in *Escherichia coli* cells, the direct involvement of this enzyme (aryl acylamidase) in the transformation of APAP, acting on the amide bond between aryl and acyl groups. Therefore, it is highly probable that the most similar proteins found in the target genomes are the enzymes responsible for catalyzing the first step of the APAP degradation pathway in the studied strains.

It is known that deaminases are responsible for the second step in the APAP biodegradation pathway. The function of deaminases is to catalyze the removal of an amino group (-NH2) from a molecule. Hence, 4-AP is turned into HQ [1]. A cytosine deaminase (Accession number: WP_130204088.1) was described for the *Pseudomonas* sp. MIL9 and used as a reference protein. Interestingly, both the CSW01 and CSW02 genomes contain a similar protein with 92 %/30 % and 89 %/30 % of coverage/identity, respectively for each bacterium and annotated as cytosine deaminase (Tables 6 and 7). Since the remarks made in the foregoing paragraphs, for proteins sharing less than 40 % sequence identity functional differences may emerge. In such instances, structural data becomes crucial to comprehend the functional similarities or dissimilarities. On the other hand, as noted by Galperin and Koonin [72], enzymes within a superfamily usually display shared sequence motifs, and essential active site residues, and often have predicted reaction mechanisms. Therefore, an analysis of the catalytic domains has been performed on the identified proteins with alignment identity percentages below 40 %. Figure S4 shows the alignment between the reference enzyme and the putative homolog proteins found, where the residues from the active site are highlighted. The alignments show conserved amino acids (highlighted in red) within the active sites related to the function under investigation in both strains. This indicates that the proteins encoded by these strains may be potential candidates for the enzymes responsible for the second step of the APAP biodegradation process. A similar study conducted by Pandey et al. [73] revealed potential genes capable of mediating the degradation of APAP, including guanidine deaminase (Accession number: WP_147428858.1). This enzyme converts 4-AP to HQ, similar to the enzyme cytosine deaminase. In the present study, the genome sequences of the CSW01 and CSW02 strains identified a guanine deaminase with 53 % and 54 % identity, respectively (Tables 6 and 7). Therefore, these are also candidates for the enzymes responsible for the second step of the APAP biodegradation process.

The subsequent step to transform HQ into hydroxyquinol is catabolized by hydroxylases, in particular ring hydroxylating oxygenase. This enzyme catalyzes the introduction of a hydroxyl group (-OH) into a substrate molecule. One aromatic-ring-hydroxylating oxygenase was reported by Musumeci et al. [74] for uncultured bacterium and it is recognized as being a key step in the aerobic biodegradation of aromatic compounds [75]. Both the α and β subunits of this enzyme (Accession numbers: AKA64675.2 and AYA78733.1) were used as a query for the search and two similar sequences of amino acids were found in each one of the target genomes, with similar levels of identity: 28 % and 32 % in the case of CSW01 strain and 30 % and 32 % in CSW02 strain (Tables 6 and 7). In the case of the α subunit, the corresponding active sites were identified on the candidate aromatic-ring-hydroxylating oxygenase protein of each studied strain (Figure S5). The alignments exhibit conserved amino acids (in red bold) in the active sites associated with the investigated function in both strains, suggesting that both encoded, despite the evolutionary differences with the enzyme described for an uncultured bacterium, and used as reference (< 40 % identity). However, the active site of the protein aromatic-ring-hydroxylating dioxygenase subunit beta is not well-defined. Interestingly, in the case of *P. extremaustralis* CSW01, these two genes appear in the contig 2 followed by each other, which gives more indications of being enzyme subunits.

Additionally, a 4-hydroxybenzoate 3-monooxygenase (Accession number: WP_024845849.1) identified in the *Paracoccus* genus was examined in the genomes under investigation. This enzyme was selected based on its involvement in the conversion of HQ to hydroxyquinol [73]. The alignments revealed a 54 % identity in the case of *P. extremaustralis* CSW01 (Table 6), a significant percentage that suggests the P-hydroxybenzoate hydroxylase gene found in this strain might be responsible for the formation of hydroxyquinol in the APAP degradation pathway. However, the genome of *S. stutzeri* CSW02 did not show evidence of the presence of 4-hydroxybenzoate 3-monooxygenase (Table 7), confirming the previously mentioned hypothesis.

The final group of proteins under investigation were dioxygenases. Several dioxygenases have been identified as the catalysts responsible for breaking open the aromatic ring during the breakdown of aromatic compounds [76,77] but their role in APAP biodegradation remains poorly understood. Rios-Miguel et al. [78] showed three possible options: (1) hydroxyquinol is transformed into 2,5-dihydroxy-6-oxo-2, 4-hexadienoic by the activity of type I extradiol dioxygenase; (2) the aromatic ring of HQ is cleaved to form 4-hydroxymuconic semialdehyde by type III extradiol dioxygenase; (3) hydroxyquinol is converted to 3-hydroxy-2,4-hexadienedioic metabolite by the action of the enzyme intradiol dioxygenase. All options were considered in this study (Tables 6 and 7 for CSW01 and CSW02, respectively). For *P. extremaustralis* CSW01 the best result in terms of identity was observed for the option of intradiol ring-cleavage dioxygenase. Namely with a catechol-1,2-dioxygenase encoded in contig 2 showing 98 % coverage and 41 % identity with both the intradiol ring-cleavage dioxygenases (Accession number: ANH99603.1) reported for *Pseudomonas koreensis* and for *Pseudomonas putida* NBRC 14164 (Accession number: BAN53997.1). In *S. stutzeri* CSW02, the best result was also for the option intradiol ring-cleavage dioxygenase, with the highest coverage (98 %) and percentage of identity (41 %) in this case just with the hydroxyquinol 1,2-dioxygenase described for *P. putida* NBRC 14164. This suggests the presence of functional intradiol ring-cleavage dioxygenase in both strains CSW01 and CSW02, and a process similar to that previously reported by Sarwade and Funde [79], in which catechol derivatives formed from the aromatic compounds' biodegradation pathways could undergo ortho or meta cleavage induced by catechol 1, 2-dioxygenase activity transforming it to cis-cis muconate.

With the goal of contributing to a broader genomic knowledge related to the biodegradation of APAP in bacteria, the reference proteins for which candidate homologs were found in the strains under study were used to search for similar genes in three bacteria known for degrading APAP and another bacteria able to degrade several aromatic compounds, whose complete genomes are available in the NCBI database. The selected bacteria for the analysis are *P. moorei* KB4, *M. yunnanensis* TJPT4, *R. wittichii* RW1, and *Paracoccus* sp. APAP_BH8 [80,17,73,13]. All of them have been described as APAP-degrading bacteria, except for *R. wittichii* RW1, which has been reported as a degrader of dibenzofuran, dibenzo-p-dioxin, polychlorinated biphenyls, and other aromatic compounds [80]. The results of the alignments between the reported degrading bacteria and reference proteins are shown in Table S4. Regarding the amidase enzyme (aryl acylamidase), several putative homologous copies were identified in *P. moorei* KB4 and *Paracoccus* sp. APAP_BH8, with wide ranges of coverage and identity. The analysis of deaminases revealed that all four bacteria present proteins to the enzyme guanine deaminase, with significant percentages of coverage and identity. The third group of proteins analyzed were hydroxylases, which exhibited greater diversity depending on the bacterial strain studied (Table S4). *P. moorei* KB4 and *R. wittichii* RW1 showed similarities with the enzyme aromatic-ring-hydroxylating oxygenase α and β subunits, as well as with the enzyme 4-hydroxybenzoate 3-monooxygenase, suggesting that both may be involved in APAP-degradation. In the case of *Paracoccus* sp. APAP_BH8, almost complete homology (98 %) was found with the protein 4-hydroxybenzoate 3-monooxygenase. However, in *M. yunnanensis* TJPT4, no homologous proteins were detected for the hydroxylases proposed for the CSW01 and CSW02 strains. Lastly, the dioxygenases, a key group in the degradation of aromatic compounds responsible for opening the aromatic ring, were

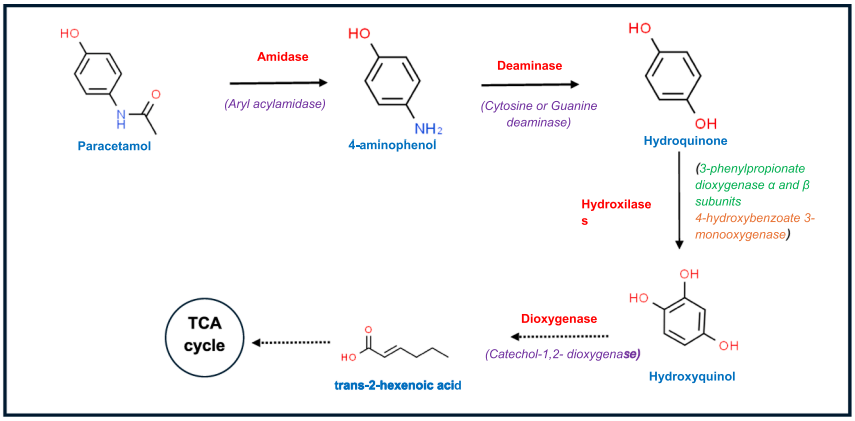

Fig. 6. Simplified paracetamol biodegradation pathway proposed for *P. extramaustralis* CSW01 and *S. stutzeri* CSW02. In brackets, enzymes as possibly responsible for catalyzing each step (in purple, those encoded by genes present in CSW01 and CSW02; in green, encoded by genes in CSW01; and in orange, encoded by genes in CSW02). Dotted lines correspond to conversions that require more than one step.

analyzed. All bacteria presented putative homologous proteins to the intradiol ring-cleavage dioxygenase. However, the percentages of identity and coverage were higher for the hydroxyquinol 1,2-dioxygenase, an intradiol ring-cleavage dioxygenase enzyme specific for hydroxyquinol, an intermediate metabolite in the degradation pathway of many aromatic compounds, including APAP [73]. In the case of *M. yunnanensis* TJPT4, the similarity was low, suggesting that this bacterium may follow an alternative degradation pathway catalyzed by an extradiol ring-cleavage dioxygenase.

After analyzing the possible candidate genes involved in the APAP degradation pathway, it was observed that the main genes amidase, hydroxylase, and dioxygenase are in the contig 2 of *P. extremaustralis* CSW01 and close to each other (peg annotations 1844, 1865, 1867, 1868). This suggests the possible presence of a cluster of genes responsible for the degradation of APAP (Fig. 6S). This hypothesis is also supported by the presence of an AmiS/UreI family transporter gene (peg 1843), which is thought to be responsible for the transport of APAP inside the cell [78], next to the aryl acylamidase amidase gene (peg 1844). Several mobile genetic elements were also found near these genes (e.g., Tn5045 resolvase, Tn3 trasposase, Transposon Tn21 modulator protein, peg. 1845, 1847, and 1849). These elements could have been responsible for the acquisition of the aforementioned gene cluster. Something similar occurs in the case of *S. stutzeri* CSW02: the analysed genes are found on the bacterial chromosome (contig 23), except for the amidase enzyme (peg 4530), which is located on a plasmid (contig 33) followed by the mobile element Tn5045 resolvase (peg 4531).

Interestingly, following the *in silico* analysis of the studied bacteria, a relationship between the detected degradative genes and the metabolites identified in this study is inferred. First, the amidase produces 4-AP, followed by the transformation of 4-AP into HQ catalyzed by a deaminase, and finally, the enzyme catechol-1,2-dioxygenase produces non-aromatic metabolic products that can lead to trans-2-hexenoic acid, ultimately destined for the TCA cycle (Fig. 6).

4. Conclusions

P. extremaustralis CSW01 and *S. stutzeri* CSW02, isolated from sewage sludge in the presence of APAP, demonstrated very high degradation capacity of this pharmaceutical in wide ranges of concentrations (10–2000 mg L^{-1}), temperature (10–40 °C) and pH (6–9, although CSW01 was very active at pH 5), exhibiting the highest capability to degrade APAP at 30 °C and pH 7.0. It indicates that both bacterial strains are very promising to be used in APAP bioremediation treatments.

Furthermore, these isolates were also able to mineralize APAP in solution although with percentages lower than 30 %, indicating that APAP metabolites should remain in solution. When the bacterial strain *M. aubagnense* HPB1.1, described as a degrader of the main APAP metabolites 4-AP and HQ, was co-inoculated with CSW01 or CSW02, the percentages of APAP mineralization increased significantly (up to 74 % and 58 %, respectively), with DT_{50} values of only 1 and 9 days, respectively. Given the scarce number of APAP mineralizing bacterial strains, the importance of these consortia for APAP mineralization in water should be highlighted.

Three metabolites (4-AP, HQ, and trans-2-hexenoic acid) were detected throughout APAP biodegradation in solution. Their removal was confirmed when the degrading strains were present, but other toxic metabolites must be formed since residual toxicity was detected until the end of the assay.

Also in sewage sludge artificially contaminated with APAP (50 mg Kg^{-1}), CSW01 and CSW02 demonstrated ability to degrade 100 % APAP in only 4 days, but mineralization was not greater than 15 % even when forming consortia with HPB1.1, concluding that some APAP metabolites may remain adsorbed on sludge.

Finally, a genome-based analysis of *P. extremaustralis* CSW01 and *S. stutzeri* CSW02 allowed to identify the genes involved in APAP degradation, and a possible pathway is proposed. Amidases, deaminases, hydroxylases and dioxygenase enzymes were identified as possibly responsible for catalyzing the different steps of the APAP biodegradation pathway. The study of the CSW01 and CSW02 genomes provides new information about the mechanism of APAP biodegradation, as the study of genes involved in the APAP degradation route is a little-known field that needs to be studied in more detail.

Environmental implication

The wide use of paracetamol (APAP) involves ecological risks, being considered an emerging pollutant. APAP excreted by humans ends up in WWTPs, where its elimination is not complete, remaining in part in the effluent treated waters (discharged into surface waters used for soil irrigation) and in part adsorbed on sewage sludge (used as fertilizer in agricultural soils). APAP bioremediation in WWTPs is the unique opportunity to remove it from both matrices before its dispersion in the environment.

Declaration of Competing Interest

The authors declare that they have no known competing financial interests or personal relationships that could have appeared to influence the work reported in this paper.

Acknowledgements

This work was supported by Junta de Andalucía (Council of Economic Transformation, Industry, Knowledge and University) under the research project PY20_01069 (FEDER Andalucía PO 2014-2020), and by Portuguese National Funds from FCT-Fundação para a Ciência e a Tecnologia, I.P., within the scope of the project PTDC/CTA-AMB/7782/2020. A.L.M. acknowledges the Margarita Salas grant to the University of Seville (funded by the European Union's Next Generation EU). A.V.O. acknowledges the Youth Employment fellowship (AND21_IRNAS_M2_158) funded by Junta de Andalucía.

Appendix A. Supporting information

Supplementary data associated with this article can be found in the online version at doi:10.1016/j.jhazmat.2024.136128.

Data Availability

Data will be made available on request.

References

[1] Grignet, R., Barros, M.G., Panatta, A.A., Bernal, S.P.F., Ottoni, J.R., Passarini, M.R. Z., Gonçalves, C., 2022. Medicines as an emergent contaminant: the review of microbial biodegration potential. Folia Microbiol 67, 157–174. https://doi.org/10.1007/s12223-021-00941-6.

[2] Nunes, B., Verde, M.F., Soares, A., 2015. Biochemical effects of the pharmaceutical drug paracetamol on Anguilla anguilla. Environ Sci Pollut Res 22, 11574–11584. https://doi.org/10.1007/s11356-015-4329-6.

[3] Parolini, M., 2020. Toxicity of the Non-Steroidal Anti-Inflammatory Drugs (NSAIDs) acetylsalicylic acid, paracetamol, diclofenac, ibuprofen and naproxen towards freshwater invertebrates: A review. Sci Total Environ 740, 140043. https://doi.org/10.1016/j.scitotenv.2020.140043.

[4] Ramos, A.S., Correia, A.T., Antunes, S.C., Gonçalves, F., Nunes, B., 2014. Effect of acetaminophen exposure in Oncorhynchusmykiss gills and liver: Detoxification mechanisms,oxidative defence system and peroxidative damage. Environ Toxicol Pharm 37 (3), 1221–1228. https://doi.org/10.1016/j.etap.2014.04.005.

[5] Morillo, E., Villaverde, J., 2017. Advanced technologies for the remediation of pesticide-contaminated soils. Sci Total Environ 586, 576–597. https://doi.org/10.1016/j.scitotenv.2017.02.020.

[6] Ahmed, S., Javed, M.A., Tanvir, S., Hameed, A., 2001. Isolation and characterization of a Pseudomonas strain that degrades 4-acetamidophenol and 4-aminophenol. Biodegradation 12, 303–309. https://doi.org/10.1023/A:1014395227133.

[7] De Gusseme, B., Vanhaecke, L., Verstraete, W., Boona, N., 2011. Degradation of acetaminophen by Delftia tsuruhatensis and Pseudomonas aeruginosa in a membrane bioreactor. Water Res 45, 1829–1837. https://doi.org/10.1016/j.watres.2010.11.040.

[8] Hu, J., Zhang, L.L., Chen, J.M., Liu, Y., 2013. Degradation of paracetamol by Pseudomonas aeruginosa strain HJ1012. J Environ Sci Health, Part A 48, 791–799. https://doi.org/10.1080/10934529.2013.744650.

[9] Palma, T.L., Donaldben, M.N., Costa, M.C., Carlier, J.D., 2018. Putative Role of Flavobacterium, Dokdonella and Methylophilus Strains in Paracetamol Biodegradation. Water Air Soil Pollut 229, 200. https://doi.org/10.1007/s11270-018-3858-2.

[10] Poddar, K., Sarkar, D., Chakraborty, D., Patil, P.B., Maity, S., Sarkar, A., 2022. Paracetamol biodegradation by Pseudomonas strain PrS10 isolated from pharmaceutical effluents. Int Biodet Biodegr 175, 105490. https://doi.org/10.1016/j.ibiod.2022.105490.

[11] Surma, R., Wojcieszynska, D., Karcz, J., Guzik, U., 2021. Effect of Pseudomonas moorei KB4 Cells' Immobilisation on Their Degradation Potential and Tolerance towards Paracetamol. Molecules 26, 820. https://doi.org/10.3390/molecules26040820.

[12] Zhang, L., Hu, J., Zhu, R., Zhou, Q.W., Chen, J.M., 2013. Degradation of paracetamol by pure bacterial cultures and their microbial consortium. Appl Microbiol Biotechnol 97, 3687–3698. https://doi.org/10.1007/s00253-012-4170-5.

[13] Żur, J., Wojcieszynska, D., Hupert-Kocurek, K., Marchlewicz, A., Guzik, U., 2018. Paracetamol e toxicity and microbial utilization. Pseudomonas moorei KB4 as a case study for exploring degradation pathway. Chemosphere 206, 192e202. https://doi.org/10.1016/j.chemosphere.2018.04.179.

[14] Chopra, S., Kumar, D., 2020. Characterization, optimization and kinetics study of acetaminophen degradation by Bacillus drentensis strain S1 and waste water degradation analysis. Bioresour Bioprocess 7, 9. https://doi.org/10.1186/s40643-020-0297-x.

[15] Chopra, S., Kumar, D., 2023. Characterization and biodegradation of paracetamol by Bacillus pumilus strain PYP2. Biocatal Biotransformation 1–12. https://doi.org/10.1080/10242422.2023.2261592.

[16] Chopra, S., Kumar, D., 2023. Characterization and biodegradation of paracetamol by biomass of Bacillus licheniformis strain PPY-2 isolated from wastewater. Rend Lince– Sci Fis e Nat 34, 491–501. https://doi.org/10.1007/s12210-023-01140-w.

[17] Palma, T., Valentine, J., Gomes, V., Faleiro, M., Costa, M., 2022. Batch Studies on the Biodegradation Potential of Paracetamol, Fluoxetine and 17-Ethinylestradiol by the Micrococcus yunnanensis Strain TJPT4 Recovered from Marine Organisms. Water 14, 3365. https://doi.org/10.3390/w14213365.

[18] Park, S., Oh, S., 2020. Detoxification and bioaugmentation potential for acetaminophen and its derivatives using Ensifer sp. isolated from activated sludge. Chemosphere 260, 127532. https://doi.org/10.1016/j.chemosphere.2020.127532.

[34] Vargas-Ordóñez, A., Aguilar-Romero, I., Villaverde, J., Madrid, F., Morillo, E., 2023. Isolation of Novel Bacterial Strains Pseudomonas extremaustralis CSW01 and Stutzerimonas stutzeri CSW02 from Sewage Sludge for Paracetamol Biodegradation. Microorganisms 11, 196. https://doi.org/10.3390/microorganisms11010196.

[20] Balakrishnan, P., Mohan, S., 2021. Treatment of triclosan through enhanced microbial biodegradation. J Hazard Mat 420, 126430. https://doi.org/10.1016/j.jhazmat.2021.126430.

[21] Xagoraraki, I., Hullman, R., Song, W., Li, H., Cai, S., Voice, T., 2008. Effect of pH on degradation of acetaminophen and production of 1,4-benzoquinone in water chlorination. J Water Supply: Res T 57 (6), 381–390. https://doi.org/10.2166/aqua.2008.095.

[22] Chen, R., Liu, K., Ma, Y., 2022. Isolation and identification of acetaminophen degrading strain Shinella sp. HZA2. J Environ Sci Health, Part B 57 (5), 333–338. https://doi.org/10.1080/03601234.2022.2054247.

[23] Mejías, C., Martín, J., Santos, J.L., Aparicio, I., Alonso, E., 2021. Occurrence of pharmaceuticals and their metabolites in sewage sludge and soil: A review on their distribution and environmental risk assessment. Trends Environ Anal Chem 30, e00125. https://doi.org/10.1016/j.teac.2021.e00125.

[24] Vaithyanathan, V.K., Cabana, H., 2021. Integrated biotechnology management of biosolids: sustainable ways to produce value—added products. Front Water 3, 729679. https://doi.org/10.3389/frwa.2021.729679.

[25] Semblante, G.U., Hai, F.I., Huang, X., Ball, A.S., Price, W.E., Nghiem, L.D., 2015. Trace organic contaminants in biosolids: Impact of conventional wastewater and sludge processing technologies and emerging alternatives. J Hazard Mat 300, 1–17. https://doi.org/10.1016/j.jhazmat.2015.06.037.

[26] European Commission (2020).Circular Economy Action Plan. (The EU's new circular action plan paves the way for a cleaner and more competitive Europe. ⟨https://environment.ec.europa.eu/strategy/circular-economy-action-plan_en⟩.

[27] Singh, V., Suthar, S., 2021. Occurrence, seasonal variation, mass loading and fate of pharmaceuticals and personal care products (PPCPs) in sewage treatment plants in cities of upper Ganges bank, India. J Water Process Eng 44, 102399. https://doi.org/10.1016/j.jwpe.2021.102399.

[28] Wei, F., Zhou, Q.W., Leng, S.Q., Zhang, L.L., Chen, J.M., 2011. Isolation, identification and biodegradation characteristics of a new bacterial strain degrading paracetamol. Environ Sci 32, 1812–1819, 02503301.

[29] Lara-Moreno, A., El-S. Ismail, F., Cox, C., Costa, M.C., Carlier, J.D., 2024. Batch studies on the biodegradation of paracetamol and 1,4-hydroquinone by novel bacterial strains isolated from extreme environmental samples and the identification of candidate catabolic genes. Appl Water Sci 14 (198). https://doi.org/10.1007/s13201-024-02264-6.

[31] López-Pacheco, I.Y., Salinas-Salazar, C., Silva-Núñez, A., Rodas-Zuluaga, L.I., Donoso-Quezada, J., Ayala-Mar, S., Barceló, D., Iqbal, H.M.N., Parra-Saldívar, R., 2019. Removal and biotransformation of 4-nonylphenol by Arthrospira maxima and Chlorella vulgaris consortium. Environ Res 179, 108848. https://doi.org/10.1016/j.envres.2019.108848.

[32] Dai, H., Gao, J., Shan, J., Lu, X., Li, D., Duan, W., Cui, Y., 2021. Pressure of high level acetaminophen on fixed biofilm and aerobic granule-based systems: Insights on nitrification performances, microbial responses and acetaminophen's biodegradation pathways. Chem Eng J 426, 131907. https://doi.org/10.1016/j.cej.2021.131907.

[33] Li, J., Ye, Q., Gan, J., 2014. Degradation and transformation products of acetaminophen in soil. Water Res 49, 44–52. https://doi.org/10.1016/j.watres.2013.11.008.

[34] FOCUS, 2006. Guidance document on estimating persistence and degradation kinetics from environmental fate studies on pesticides in EU registration. Report of the FOCUS work group on degradation kinetics. EC Doc Ref Sanco/10058/2005 Version 2 (0), 434. ⟨https://esdac.jrc.ec.europa.eu/public_path/projects_data/focus/dk/docs/finalreportFOCDegKinetics.pdf⟩.

[35] Beulke, S., van Beinum, W., Brown, C.D., Mitchell, M., Walker, A., 2005. Evaluation of Simplifying Assumptions on Pesticide Degradation in Soil. J Environ Qual 34 (6), 1933–1943. https://doi.org/10.2134/jeq2004.0460.

[36] Persoone, G., Marsalek, B., Blinova, I., Torokne, A., Zarina, D., Manusadzianas, L., Nalecz-Jawecki, G., Tofan, L., Stepanova, N., Tothova, L., Kolar, B., 2003. A practical and user-friendly toxicity classification system with microbiotests for natural waters and wastewa-ters. Environ Toxicol 18 (6), 395–402. https://doi.org/10.1002/tox.10141.

[37] Jones, P., Binns, D., Chang, H.Y., Fraser, M., Li, W., McAnulla, C., McWilliam, H., Maslen, J., Mitchell, A., Nuka, G., Pesseat, S., Quinn, A.F., Sangrador-Vegas, A., Scheremetjew, M., Yong, S.Y., Lopez, R., Hunter, S., 2014. InterProScan 5: genome-scale protein function classification. Bioinformatic 30 (9), 1236–1240. https://doi.org/10.1093/bioinformatics/btu031.

[38] Alexander, M., 1999. Biodegradation and Bioremediation, 2nd ed..,. Academic Press,, San Diego, CA, USA, pp. 92101–94495. ISBN 978-0-12-049861-1.

[39] Żur, J., Piński, A., Marchlewicz, A., Hupert-Kocurek, K., Wojcieszyńska, D., Guzik, U., 2018. Organic micropollutants paracetamol and ibuprofen—toxicity,

biodegradation, and genetic background of their utilization by bacteria. Environ Sci Pollut Res 25, 21498–21524. https://doi.org/10.1007/s11356-018-2517-x.
[40] Moon, S., Ham, S., Jeong, J., Ku, H., Kim, H., Lee, C., 2023. Temperature Matters: Bacterial Response to Temperature Change. J Microbiol 61, 343–357. https://doi.org/10.1007/s12275-023-00031-x.
[41] Das, N., Chandran, P., 2011. Microbial Degradation of Petroleum Hydrocarbon Contaminants: An Overview. Biotech Res Int 13, 941810. https://doi.org/10.4061/2011/941810.
[42] Zhang, Y., Gross, C.A., 2021. Cold shock response in bacteria. Annu Rev Genet 55, 377–400. https://doi.org/10.1146/annurev-genet-071819-031654.
[43] López, N.I., Pettinari, M.J., Stackebrandt, E., Tribelli, P.M., Potter, M., Steinbüchel, A., Méndez, B.S., 2009. Pseudomonas extremaustralis sp. nov., a Poly (3-hydroxybutyrate) Producer Isolated from an Antarctic Environment. Curr Microbiol 59, 514–519. https://doi.org/10.1007/s00284-009-9469-9.
[44] Tribelli, P.M., Solar Venero, E.C., Ricardi, M.M., Gómez-Lozano, M., Raiger Iustman, L.J., Molin, S., López, N., 2015. Novel essential role of ethanol oxidation genes at low temperature revealed by transcriptome analysis in the Antarctic bacterium pseudomonas extremaustralis. PLoS ONE 10 (12), e0145353. https://doi.org/10.1371/journal.pone.0145353.
[45] Ayub, N.D., Tribelli, P.M., López, N.I., 2009. Polyhydroxyalkanoates are essential for maintenance of redox state in the Antarctic bacterium Pseudomonas sp. 14-3 during low temperature adaptation. Extremophiles 13, 59–66. https://doi.org/10.1007/s00792-008-0197-z.
[46] Wolski, E.A., Murialdo, S.E., Gonzale, J.F., 2006. Effect of pH and inoculum size on pentachlorophenol degradation by Pseudomonas sp. Water SA 32 (1). https://doi.org/10.4314/wsa.v32i1.5228.
[47] Chopra, S., Kumar, D., 2020. Biodegradation and kinetic analysis of acetaminophen with co-culture of bacterial strains isolated from sewage wastewater. Curr Microbiol 77 (10), 3147–3157. https://doi.org/10.1007/s00284-020-02137-6.
[48] Peterson, S.B., Bertolli, S.K., Mougous, J.D., 2020. The Central Role of Interbacterial Antagonism in Bacterial Life. Curr Biol 30 (19), 1203–1214. https://doi.org/10.1016/j.cub.2020.06.103.
[49] Lara-Moreno, A., Morillo, E., Merchán, F., Madrid, F., Villaverde, J., 2022. Bioremediation of a trifluralin contaminated soil using bioaugmentation with novel isolated bacterial strains and cyclodextrin. Sci Total Environ 840, 156695. https://doi.org/10.1016/j.scitotenv.2022.156695.
[50] Villaverde, J., Rubio-Bellido, M., Lara-Moreno, A., Merchán, F., Morillo, E., 2018. Combined use of microbial consortia isolated from different agricultural soils and cyclodextrin as a bioremediation technique for herbicide contaminated soils. Chemosphere 193, 118–125. https://doi.org/10.1016/j.chemosphere.2017.10.172.
[51] Lara-Moreno, A., Morillo, E., Merchán, F., Villaverde, J., 2021. A comprehensive feasibility study of effectiveness and environmental impact of PAH bioremediation using an indigenous microbial degrader consortium and a novel strain stenotrophomonas maltophilia CPHE1 isolated from an industrial polluted soil. J Environ Manag 289, 112512. https://doi.org/10.1016/j.jenvman.2021.112512.
[52] Aguilar-Romero, I., Madrid, F., Villaverde, J., Morillo, E., 2024. Ibuprofen-enhanced biodegradation in solution and sewage sludge by a mineralizing microbial consortium. Shift in associated bacterial communities. J Hazard Mat 46415, 132970. https://doi.org/10.1016/j.jhazmat.2023.132970.
[53] Zimmermann, P., Curtis, N., 2017. Antimicrobial effects of antipyretics. Antimicrob Agents Chemother 61, e02268-16. https://doi.org/10.1128/AAC.02268-16.
[54] Razafintsalama, V., Sarter, S., Mambu, L., Randrianarivo, R., Petit, T., Rajaonarison, J.F., Mertz, C., Rakoto, D., Jeannoda, V., 2013. Antimicrobial activities of Dilobeia thouarsii Roemer and Schulte, a traditional medicinal plant from Madagascar. South Afr J Bot 87, 1–3. https://doi.org/10.1016/j.sajb.2013.02.171.
[55] Lana, E.J., Carazza, F., Takahashi, J.A., 2006. Antibacterial evaluation of 1,4-benzoquinone derivatives. J Agric Food Chem 54, 2053–2056. https://doi.org/10.1021/jf052407z.
[56] Enguita, F.J., Leitão, A.L., 2013. Hydroquinone: Environmental pollution, toxicity, and microbial answers. Biomed Res Int 2013, 542168. https://doi.org/10.1155/2013/542168.
[57] Ivshina, I.B., Rychkova, M.I., Vikhareva, E.V., Chekryshkina, L.A., Mishenina, I.I., 2006. Catalysis of the biodegradation of unusable medicines by *Alkanotrophic Rhodococci*. Appl Biochem Microbiol 42, 392–395. https://doi.org/10.1134/S0003683806040090.
[58] Takenaka, S., Okugawa, S., Kadowaki, M., Murakami, S., Aoki, K., 2003. The metabolic pathway of 4-aminophenol in Burkholderia sp. Strain AK-5 differs from that of aniline and aniline with C-4 substituents. Appl Environ Microbiol 69, 5410–5413. https://doi.org/10.1128/AEM.69.9.5410-5413.2003.
[59] Jiang, Y., Brassingtona, K.J., Prpich, G., Paton, G.I., Semple, K.T., Pollard, S.J.T., Coulona, F., 2016. Insights into the biodegradation of weathered hydrocarbons in contaminated soils by bioaugmentation and nutrient stimulation. Chemosphere 161, 300–307. https://doi.org/10.1016/j.chemosphere.2016.07.032.
[60] Lara-Moreno, A., Morillo, E., Villaverde, J., 2022. Enhanced biodegradation of phenylurea herbicides by Ochrobactrum anthrophi CD3 assessment of its feasibility in Diuron-contaminated soils. Int J Environ Res Public Health 19, 1365. https://doi.org/10.3390/ijerph19031365.
[61] Palma, T.L., Magno, G., Costa, M.C., 2021. Biodegradation of Paracetamol by Some Gram-Positive Bacterial Isolates. Curr Microbiol 78 (7), 2774–2786. https://doi.org/10.1007/s00284-021-02543-4.
[62] Liu, Y., Chang, H., Li, Z., Feng, Y., Cheng, D., Xue, J., 2017. Biodegradation of gentamicin by bacterial consortia AMQD4 in synthetic medium and raw gentamicin sewage. Sci Rep 7, 11004. https://doi.org/10.1038/s41598-017-11529-x.
[63] Wu, S., Zhang, L., Chen, J., 2012. Paracetamol in the environment and its degradation by microorganisms. Appl Microbiol Biotechnol 96, 875–884. https://doi.org/10.1007/s00253-012-4414-4.
[64] Rost, B., 1999. Twilight zone of protein sequence alignments. Prot Eng 12 (2), 85–94. ⟨https://academic.oup.com/peds/article/12/2/85/1550637⟩.
[65] Todd, A.E., Orengo, C.A., Thornton, J.M., 2001. Evolution of function in protein superfamilies, from a structural perspective. J Mol Biol 307 (4), 1113–1143. https://doi.org/10.1006/jmbi.2001.4513.
[13] Rios-Miguel, A.B., Smith, G.J., Cremers, G., van Alen, T., Jetten, M.S.M., Op den Camp, H.J.M., Welte, C.U., 2022. Microbial paracetamol degradation involves a high diversity of novel amidase enzyme candidates. Water Res 16, 100152. https://doi.org/10.1016/j.wroa.2022.100152.
[67] Ko, H.J., Lee, E.W., Bang, W.G., Lee, C.K., Kim, K.H., Choi, G., 2010. Molecular characterization of a novel bacterial aryl acylamidase belonging to the amidase signature enzyme family. Mol Cells 29, 485–492. https://doi.org/10.1007/s10059-010-0060-9.
[68] Zhang, J., Yin, J.G., Hang, B.J., He, J., Zhou, S., Li, S., 2012. Cloning of a novel arylamidase gene from Paracoccus SP. strain FLN-7 that hydrolyzes amide pesticides. Appl Environ Microbiol 78, 4848–4855. https://doi.org/10.1128/aem.00320-12.
[69] Zhang, L., Hu, Q., Hang, P., Zhou, X., Jiang, J., 2019. Characterization of an arylamidase from a newly isolated propanil-transforming strain of Ochrobactrum SP. PP-2. Ecotoxicol Environ Saf 167, 122–129. https://doi.org/10.1016/j.ecoenv.2018.09.127.
[70] Chen, Q., Chen, K., Ni, H., Zhuang, W., Wang, H., Zhu, J., He, Q., He, J., 2016. A novel amidohydrolase (DmhA) from Sphingomonas sp. that can hydrolyze the organophosphorus pesticide dimethoate to dimethoate carboxylic acid and methylamine. Biotechnol Lett 38, 703–710. https://doi.org/10.1007/s10529-015-2027-6.
[71] Ko, H.J., Bang, W.G., Kim, K.H., Choi, I.G., 2012. Production of p-acetaminophenol by whole-cell catalysis using Escherichia coli overexpressing bacterial aryl acylamidase. Biotechnol Lett 34, 677–682. https://doi.org/10.1007/s10529-011-0811-5.
[72] Galperin, M.Y., Koonin, E.V., 2012. Divergence and convergence in enzyme evolution. J Biol Chem 287 (1), 21–28. https://doi.org/10.1074/jbc.R111.241976.
[73] Pandey, B., Pandey, A.K., Tripathi, K., Dubey, S.K., 2024. Biodegradation of acetaminophen: Microcosm centric genomic-proteomic-metabolomics evidences. Biosour Biotechn 401, 130732. https://doi.org/10.1016/j.biortech.2024.130732.
[74] Musumeci, M.A., Loviso, C.L., Lozada, M., Ferreira, F.V., Dionisi, H.M., 2019. Substrate specificities of aromatic ring-hydroxylating oxygenases of an uncultured gammaproteobacterium from chronically-polluted subantarctic sediments. Int Biodeterior Biodegrad 137, 127–136. https://doi.org/10.1016/j.ibiod.2018.12.005.
[75] Khara, P., Roy, M., Chakraborty, J., Ghosal, D., Dutta, T.K., 2014. Functional characterization of diverse ring-hydroxylating oxygenases and induction of complex aromatic catabolic gene clusters insphingobiumSP. PNB. FEBS Open Bio 4, 290–300. https://doi.org/10.1016/j.fob.2014.03.001.
[76] Ferraroni, M., Da Vela, S., Kolvenbach, B.A., Corvini, P.F.X., Scozzafava, A., 2017. The crystal structures of native hydroquinone 1,2-dioxygenase from Sphingomonas sp. TTNP3 and of substrate and inhibitor complexes. Biochim Biophys Acta, Proteins Proteom 1865, 520–530. https://doi.org/10.1016/j.bbapap.2017.02.013.
[77] Kolvenbach, B.A., Lenz, M., Benndorf, D., Rapp, E., Fousek, J., Vlcek, C., Schäffer, A., Gabriel, F., Kohler, H.P.E., Corvini, P.F.X., 2011. Purification and characterization of hydroquinone dioxygenase from Sphingomonas sp. strain TTNP3. AMB Expr 1, 8. https://doi.org/10.1186/2191-0855-1-8.
[79] Sarwade, V., Funde, S., 2022. Biotransformation of nitro aromatic amines in artificial alkaline habitat by Pseudomonas DL17. Environ Anal Health Toxicol 37, e2022001. https://doi.org/10.5620/eaht.2022001.
[80] Hassan, H.A., dEnza, M., Armengaud, J., Pieper, D.H., 2022. Biochemical and genetic characterization comparison of four extradiol dioxygenases in Rhizorhabdus wittichii RW1. Appl Microbiol Biotechnol 106, 5539–5550. https://doi.org/10.1007/s00253-022-12099-3.